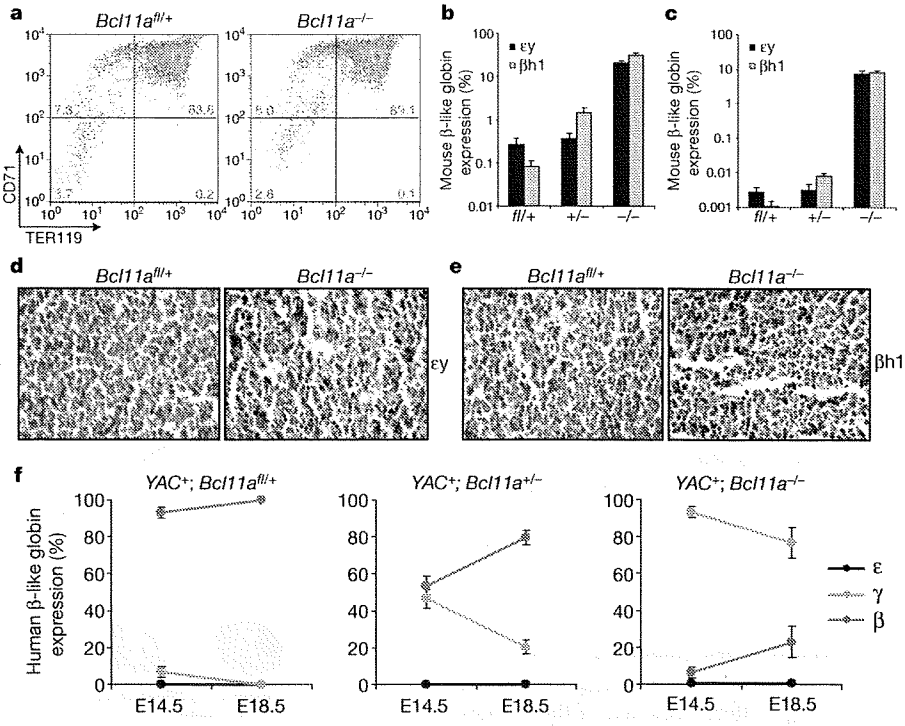

Figure 4 | *Bcl11a*$^{-/-}$ mice fail to silence the expression of mouse embryonic β-like globins and human γ-globin genes. **a**, The CD71 and TER119 expression pattern is shown for fetal liver cells from E14.5 embryos, revealing grossly normal erythropoiesis with these phenotypic markers. The mean percentages for the populations in each quadrant are shown in red ($n = 6$ for *Bcl11a*$^{fl/+}$ controls, $n = 4$ for *Bcl11a*$^{-/-}$ mutants). $P > 0.1$, using a two-sided *t*-test for all gated populations analysed. **b**, The expression of the embryonic globins is shown as a percentage of total mouse β-like globins for control mice (*fl*/+), *Bcl11a* heterozygous (+/−), and null mice (−/−) at E14.5 ($n = 10$, 14 and 11, respectively). **c**, The expression of the embryonic globins is shown as a percentage of the total mouse β-like globins at E18.5 ($n = 9$, 9 and 7, respectively). **d**, IHC was performed on E14.5 fetal livers from *Bcl11a*$^{fl/+}$ and *Bcl11a*$^{-/-}$ animals for the embryonic globin εy. Representative sections at ×40 magnification with a ×10 objective lens are shown. **e**, Similar IHC staining was performed for βh1 globin. In both cases robust expression is seen in the scattered erythroblasts of the fetal liver in *Bcl11a*$^{-/-}$ but not control mice. **f**, Expression of human β-globin locus genes is shown for animals with the various *Bcl11a* genotypes in the presence of the β-locus YAC transgene (*YAC*$^{+}$) at E14.5 ($n = 4$, 6 and 4 for the *Bcl11a*$^{fl/+}$, *Bcl11a*$^{+/-}$ and *Bcl11a*$^{-/-}$ animals, respectively) and E18.5 ($n = 4$, 7 and 4). All γ- and β-globin levels for the different genotypes are significantly different ($P < 1 \times 10^{-5}$, two-sided *t*-test). All data are plotted as the mean ± s.d. of the measurement.

2,600- and 7,600-fold compared to controls (Fig. 4c). To determine the cellular distribution of the mouse embryonic globins, we performed IHC. Using this approach we found that εy and βh1 globins were robustly expressed in definitive erythroid cells (Fig. 4d, e and Supplementary Fig. 9), whereas normally these embryonic globins are confined to the primitive erythroid lineage[5] (Fig. 3b).

Silencing of human γ-globin expression depends on BCL11A

We then examined the consequence of BCL11A loss on the regulation of human globin genes in the β-locus mice. By introducing the β-locus transgene into the knockout environment, we found that in the absence of BCL11A, developmental silencing of the γ-globin genes is markedly impaired in the definitive erythroid lineage (Fig. 4f and Supplementary Fig. 10). In *Bcl11a*$^{-/-}$, *Bcl11a*$^{+/-}$ and littermate control mice, γ-globin RNA comprised 76%, 20% and 0.24% of total β-like globin gene RNA at E18.5, respectively (Fig. 4f and Supplementary Fig. 10). Relaxation of γ-globin gene silencing in *Bcl11a*$^{+/-}$ heterozygotes is consistent with the genetic association of BCL11A and HbF levels, and extends our previous observations using knockdown approaches in human cells[23] that together point to BCL11A as a quantitative regulator of γ-globin expression. The failure of γ-globin gene silencing in the face of otherwise ostensibly normal erythropoiesis provides compelling evidence that BCL11A is an important regulator of the globin switches in mouse and human ontogeny.

Concluding remarks

Taken together, our findings demonstrate how changes in the expression of a single *trans*-acting factor over the course of evolution may lead to altered developmental gene expression. We have shown that *cis*-elements in the human β-globin locus are insufficient to recapitulate proper developmental regulation in a mouse context. Previously it has been postulated that the evolution of β-like globin gene expression is largely mediated through changes in *cis*-elements[27]. Our findings argue persuasively that changes in *trans*-acting factors may exert notable effects on gene switching during development. BCL11A acts to silence the embryonic genes in mouse definitive erythroid cells, in contrast to its role in humans where it acts to silence γ-globin expression after birth. Moreover, we show that BCL11A is a powerful regulator of the species-divergent globin switches by demonstrating that the γ-globin gene escapes proper developmental silencing in a mouse *trans*-acting *Bcl11a*$^{-/-}$ environment. Our findings suggest a model in which one (or more) *trans*-acting silencers of the embryonic globin genes, initially expressed throughout definitive erythropoiesis, have been altered during primate evolution, such that their expression is shifted to a later phase of definitive erythropoiesis, allowing for the evolution of a unique fetal haemoglobin expression stage. We have shown here that BCL11A represents one of the major factors regulating this switch. These findings allow for simplification of molecular models accounting for this critical developmental transition. This work provides not only unique insights into how alterations in gene expression occur in the course of evolution, but also reveals further mechanistic clues to the clinically important fetal-to-adult haemoglobin switch in humans.

METHODS SUMMARY

All experiments performed with the β-locus, K-RasG12D, *Bcl11a*$^{-/-}$, Gata1-Cre, and Mx1-Cre mice were approved by the Children's Hospital Boston Animal Ethics Committee and the Ethics Committee of the Fred Hutchinson Cancer

Research Center. The analysis of adult and developmental haematopoiesis/erythropoiesis was performed using FACS-based phenotypic and morphological approaches as described[25,26]. Quantitative PCR and western blotting were carried out as described[23,25]. RNA primary transcript fluorescence *in situ* hybridization was performed with some modification of published protocols[16,17].

Full Methods and any associated references are available in the online version of the paper at www.nature.com/nature.

Received 5 April; accepted 30 June 2009.
Published online 5 August 2009.

1. Carroll, S. B. Evo-devo and an expanding evolutionary synthesis: a genetic theory of morphological evolution. *Cell* **134,** 25–36 (2008).
2. Hoekstra, H. E. & Coyne, J. A. The locus of evolution: evo devo and the genetics of adaptation. *Evolution* **61,** 995–1016 (2007).
3. Wallace, H. A. *et al.* Manipulating the mouse genome to engineer precise functional syntenic replacements with human sequence. *Cell* **128,** 197–209 (2007).
4. Wilson, M. D. *et al.* Species-specific transcription in mice carrying human chromosome 21. *Science* **322,** 434–438 (2008).
5. McGrath, K. & Palis, J. Ontogeny of erythropoiesis in the mammalian embryo. *Curr. Top. Dev. Biol.* **82,** 1–22 (2008).
6. Wijgerde, M., Grosveld, F. & Fraser, P. Transcription complex stability and chromatin dynamics *in vivo*. *Nature* **377,** 209–213 (1995).
7. Peterson, K. R., Navas, P. A., Li, Q. & Stamatoyannopoulos, G. LCR-dependent gene expression in β-globin YAC transgenics: detailed structural studies validate functional analysis even in the presence of fragmented YACs. *Hum. Mol. Genet.* **7,** 2079–2088 (1998).
8. Porcu, S. *et al.* The human β globin locus introduced by YAC transfer exhibits a specific and reproducible pattern of developmental regulation in transgenic mice. *Blood* **90,** 4602–4609 (1997).
9. Peschle, C. *et al.* Haemoglobin switching in human embryos: asynchrony of ζ→α and ε→γ-globin switches in primitive and definite erythropoietic lineage. *Nature* **313,** 235–238 (1985).
10. Sloane-Stanley, J., Roberts, N. A., Olivieri, N., Weatherall, D. J. & Wood, W. G. Globin gene expression in Hb Lepore-BAC transgenic mice. *Br. J. Haematol.* **135,** 735–737 (2006).
11. Pace, B., Li, Q., Peterson, K. & Stamatoyannopoulos, G. α-Amino butyric acid cannot reactivate the silenced γ gene of the β locus *YAC* transgenic mouse. *Blood* **84,** 4344–4353 (1994).
12. Papayannopoulou, T., Torrealba de Ron, A., Veith, R., Knitter, G. & Stamatoyannopoulos, G. Arabinosylcytosine induces fetal hemoglobin in baboons by perturbing erythroid cell differentiation kinetics. *Science* **224,** 617–619 (1984).
13. Weatherall, D. J. *et al.* Foetal erythropoiesis in human leukaemia. *Nature* **257,** 710–712 (1975).
14. Kingsley, P. D. *et al.* "Maturational" globin switching in primary primitive erythroid cells. *Blood* **107,** 1665–1672 (2006).
15. Fraser, S. T., Isern, J. & Baron, M. H. Maturation and enucleation of primitive erythroblasts during mouse embryogenesis is accompanied by changes in cell-surface antigen expression. *Blood* **109,** 343–352 (2007).
16. Ragoczy, T., Bender, M. A., Telling, A., Byron, R. & Groudine, M. The locus control region is required for association of the murine β-globin locus with engaged transcription factories during erythroid maturation. *Genes Dev.* **20,** 1447–1457 (2006).
17. Trimborn, T., Gribnau, J., Grosveld, F. & Fraser, P. Mechanisms of developmental control of transcription in the murine α- and β-globin loci. *Genes Dev.* **13,** 112–124 (1999).
18. Chada, K., Magram, J. & Costantini, F. An embryonic pattern of expression of a human fetal globin gene in transgenic mice. *Nature* **319,** 685–689 (1986).
19. Uda, M. *et al.* Genome-wide association study shows *BCL11A* associated with persistent fetal hemoglobin and amelioration of the phenotype of β-thalassemia. *Proc. Natl Acad. Sci. USA* **105,** 1620–1625 (2008).
20. Lettre, G. *et al.* DNA polymorphisms at the *BCL11A, HBS1L-MYB,* and β-*globin* loci associate with fetal hemoglobin levels and pain crises in sickle cell disease. *Proc. Natl Acad. Sci. USA* **105,** 11869–11874 (2008).
21. Menzel, S. *et al.* A QTL influencing F cell production maps to a gene encoding a zinc-finger protein on chromosome 2p15. *Nature Genet.* **39,** 1197–1199 (2007).
22. Sedgewick, A. E. *et al. BCL11A* is a major HbF quantitative trait locus in three different populations with β-hemoglobinopathies. *Blood Cells Mol. Dis.* **41,** 255–258 (2008).
23. Sankaran, V. G. *et al.* Human fetal hemoglobin expression is regulated by the developmental stage-specific repressor *BCL11A*. *Science* **322,** 1839–1842 (2008).
24. Liu, P. *et al.* Bcl11a is essential for normal lymphoid development. *Nature Immunol.* **4,** 525–532 (2003).
25. Sankaran, V. G., Orkin, S. H. & Walkley, C. R. *Rb* intrinsically promotes erythropoiesis by coupling cell cycle exit with mitochondrial biogenesis. *Genes Dev.* **22,** 463–475 (2008).
26. Zhang, J., Socolovsky, M., Gross, A. W. & Lodish, H. F. Role of Ras signaling in erythroid differentiation of mouse fetal liver cells: functional analysis by a flow cytometry-based novel culture system. *Blood* **102,** 3938–3946 (2003).
27. Johnson, R. M. *et al.* Phylogenetic comparisons suggest that distance from the locus control region guides developmental expression of primate β-type globin genes. *Proc. Natl Acad. Sci. USA* **103,** 3186–3191 (2006).

Supplementary Information is linked to the online version of the paper at www.nature.com/nature.

Acknowledgements We are grateful to K. Peterson and H. Fedosyuk for providing β-locus mice, K. Gaensler for the A20 and A85 strains of β-locus mice, and T. Jacks for providing the K-RasG12D mice. We thank J. Palis and P. Kingsley for providing mouse embryonic globin antibodies, H. Mikkola and B. Van Handel for providing sorted human samples, and R. Byron and A. Telling for technical support. We thank L. Zon, K. McGrath, P. Kingsley, J. Palis, M. Kowalczyk and T. Menne for advice and discussions. This work was supported by funding from the National Institute of Diabetes and Digestive and Kidney Diseases (NIDDK) and the National Heart, Lung, and Blood Institute (NHLBI) of the National Institutes of Health (NIH) (S.H.O. and M.G.) and the National Cancer Institute (P.W.T.). S.H.O. is an Investigator of the Howard Hughes Medical Institute (HHMI). C.R.W. is a special fellow of the Leukemia & Lymphoma Society. T.R. is supported by a fellowship from the American Society of Hematology. J.X. is an HHMI fellow of the Helen Hay Whitney Foundation. V.G.S. is supported by a Medical Scientist Training Program Award from the NIH and G.C.I. is supported by a NCI postdoctoral fellowship.

Author Contributions V.G.S., J.X. and S.H.O. conceived the study design. V.G.S., J.X., T.R., C.R.W., Y.F., M.I. and M.A.B. performed the experiments. V.G.S., J.X., T.R., C.R.W., M.G., M.A.B. and S.H.O. analysed data. G.C.I., S.D.M. and P.W.T. developed and contributed a new mouse line. V.G.S., J.X. and S.H.O. wrote the paper. All authors read, helped revise, and approved the manuscript.

Author Information Reprints and permissions information is available at www.nature.com/reprints. The authors declare competing financial interests: details accompany the full-text HTML version of the paper at www.nature.com/nature. Correspondence and requests for materials should be addressed to S.H.O. (stuart_orkin@dfci.harvard.edu).

METHODS

Experimental animals. The wild-type β-globin locus YAC transgenic (β-YAC) mouse strains that were used in this study show a similar pattern of human globin gene expression and are representative of the various strains of transgenic mice harbouring the entire human β-globin locus[7,8,28–31]. One transgenic mouse line was provided by K. Peterson and was created with the insertion of a 213 kilobase (kb) YAC containing the entire intact human β-globin locus and has been described and characterized previously[7,28,29]. This β-YAC line contains three intact copies of the human β-globin locus integrated at a single genomic locus. Two β-YAC lines (A20 and A85) containing a single copy of a ~150-kb β-globin locus YAC were also used in this study and have been described previously[8] (provided by K. Gaensler). These transgenes were maintained in the hemizygous state. The animals were maintained on a pure C57Bl/6 background for all experiments involving adult haematopoietic analysis. A juvenile myelomonocytic leukaemia-type myeloproliferative disorder was induced by crossing the Mx1-Cre line with the K-RasG12D conditional allele[32,33], along with the β-YAC transgene from K. Peterson. Congenic B6.SJL-PtprcaPep3b/BoyJ (Ptprca or CD45.1) mice were purchased from Taconic Farms or The Jackson Laboratory. Mice containing a *Bcl11a* floxed allele (with *loxP* sites flanking exon 1) were created by gene targeting approaches and will be described in future work (G.C.I., S.D.M. and P.W.T., unpublished observations). To obtain the *Bcl11a*-null allele, these mice were crossed with GATA1-Cre mice and screened for germline deletions[34,35]. All experiments were performed with the approval of the Children's Hospital Boston Animal Ethics Committee and the Ethics Committee of the Fred Hutchinson Cancer Research Center.

Adult haematopoietic analysis. Analyses of adult haematology, bone marrow transplants and 5-fluorouracil induction were performed as described previously[25,36]. Whole blood was analysed on a Beckman Coulter AcT^{10} haematological analyser. Recipient (CD45.1) mice were irradiated with a total of 10.5 Gy γ-radiation (5 Gy and 5.5 Gy, 3 h apart) on the day of transplantation. Whole bone marrow was isolated and pooled from β-YAC mice. A total of 2×10^6 cells per mouse were retro-orbitally injected into recipients. RNA was obtained from blood using the QiaAmp Blood Mini Kit (Qiagen), and quantitative reverse trasnscriptase PCR (qRT–PCR) was performed as described[23,25] using the human globin gene primers listed or previously reported murine primers[14]. The human globin gene primers were: ε-globin exon 1 forward, 5′-GAGAGGCAGCAGCA CATATC-3′; ε-globin exon 2 reverse, 5′-CAGGGGTAAACAACGAGGAG-3′; γ-globin exon 2 forward, 5′-TGGATGATCTCAAGGGCAC-3′; γ-globin exon 3 reverse, 5′-TCAGTGGTATCTGGAGGACA-3′; β-globin exon 1 forward, 5′-CT GAGGAGAAGTCTGCCGTTA-3′; and β-globin exon 2 reverse, 5′-AGCAT CAGGAGTGGACAGAT-3′. The mouse globin gene primers were: εy globin exon 1 forward, 5′-TGGCCTGTGGAGTAAGGTCAA-3′; εy globin exon 2 reverse, 5′-GAAGCAGAGGACAAGTTCCCA-3′; βh1 globin exon 2 forward, 5′-TGGACAACCTCAAGGAGACC-3′; βh1 globin exon 3 reverse, 5′-ACCTCT GGGGTGAATTCCTT-3′; βmajor/βminor globins exon 2 forward, 5′-TTTA ACGATGGCCTGAATCACTT-3′; and βmajor/βminor globins exon 3 reverse, 5′-CAGCACAATCACGATCATATTGC-3′. The mouse *Bcl11a* qRT–PCR primers were forward, 5′-AACCCCAGCACTTAAGCAAA-3′; and reverse, 5′- ACAGGTGAGAAGGTCGTGGT-3′.

Developmental haematopoietic analysis. Embryos were obtained from timed matings, bled and TER119-positive cells were sorted on the basis of forward and side scatter, similar to what has been previously described[14]. Cells were maintained in PBS with 5% FCS. Unfractionated heparin in PBS was added to this solution to a final concentration of 12.5 μg ml^{-1}. IHC using an anti-HbF polyclonal antibody was performed on fixed paraffin-embedded sections as described[37]. The fetal livers of E13.5 murine embryos were dissected and a single-cell suspension was created. Similarly, bone marrow cells were collected as has been described previously from mice[25]. In both cases, the cells were labelled with TER119 and CD71, as well as with 7-AAD. The TER119$^+$/CD71$^+$ populations were sorted as described previously[25]. Stage-matched human samples were obtained and sorted as previously described[23]. These human samples were provided by H. Mikkola and B. Van Handel.

Western blot analysis of BCL11A. Expression of BCL11A was performed using antibody 14B5 (Abcam), as described previously[23]. Expression of GAPDH was assessed as a standard using rabbit polyclonal antibody FL-335 (Santa Cruz Biotechnology).

RNA primary transcript FISH. PT-FISH was largely performed as previously described[6,16] with some modifications. Before hybridization, the slides were equilibrated in 50% formamide, 2× SSC, pH 7.0. Single-stranded DNA probes against the introns of the murine α- and εy- and human γ- and β-globin genes were generated by *in vitro* transcription of cloned intron fragments, followed by reverse transcription and inclusion of DIG-11-dUTP, biotin-16-dUTP (Roche) or DNP-11-dUTP (Perkin Elmer) in the reactions as described[38]. Labelled probes were hybridized to the cells in 50% formamide, 10% dextran sulphate, 2× SSC, 5 mM ribonucleotide vanadate complex, 0.05% BSA, 0.1 mg ml^{-1} Cot-1 DNA, 1 μg μl^{-1} *Escherichia coli* tRNA. The probes were heat denatured at 80 °C for 5 min, pre-annealed at 37 °C, and then hybridized overnight at 37 °C in a humid chamber. Slides were washed in 50% formamide, 2× SSC, pH 7 at 37 °C, rinsed in 2× SSC and blocked in 145 mM NaCl, 0.1 M Tris, pH 7.5, 2% BSA, 2 mM ribonucleotide vanadate complex. Primary transcript foci were detected by indirect immunofluorescence with Cy3-, Alexa Fluor 488- and 647-conjugated antibodies including one or two layers of signal amplification, as described[17].

FISH image acquisition and analysis. Image stacks (*Z* sections spaced 0.25 μm apart) were captured on an Olympus IX71 microscope (Olympus objective ×100/1.40, UPLS Apo) equipped with a cooled CCD camera using Deltavision SoftWorx software (Applied Precision). The presence of the globin gene primary transcripts was determined in two-dimensional projections of the *Z* stacks using Photoshop (Adobe). Between 100–200 nuclei were analysed for each probe set and maturation stage.

28. Peterson, K. R. *et al.* Transgenic mice containing a 248-kb yeast artificial chromosome carrying the human β-globin locus display proper developmental control of human globin genes. *Proc. Natl Acad. Sci. USA* **90**, 7593–7597 (1993).
29. Harju, S., Navas, P. A., Stamatoyannopoulos, G. & Peterson, K. R. Genome architecture of the human β-globin locus affects developmental regulation of gene expression. *Mol. Cell. Biol.* **25**, 8765–8778 (2005).
30. Gaensler, K. M., Kitamura, M. & Kan, Y. W. Germ-line transmission and developmental regulation of a 150-kb yeast artificial chromosome containing the human β-globin locus in transgenic mice. *Proc. Natl Acad. Sci. USA* **90**, 11381–11385 (1993).
31. Strouboulis, J., Dillon, N. & Grosveld, F. Developmental regulation of a complete 70-kb human β-globin locus in transgenic mice. *Genes Dev.* **6**, 1857–1864 (1992).
32. Chan, I. T. *et al.* Conditional expression of oncogenic *K-ras* from its endogenous promoter induces a myeloproliferative disease. *J. Clin. Invest.* **113**, 528–538 (2004).
33. Braun, B. S. *et al.* Somatic activation of oncogenic *Kras* in hematopoietic cells initiates a rapidly fatal myeloproliferative disorder. *Proc. Natl Acad. Sci. USA* **101**, 597–602 (2004).
34. Garrick, D. *et al.* Loss of Atrx affects trophoblast development and the pattern of X-inactivation in extraembryonic tissues. *PLoS Genet.* **2**, e58 (2006).
35. Jasinski, M., Keller, P., Fujiwara, Y., Orkin, S. H. & Bessler, M. GATA1-Cre mediates *Piga* gene inactivation in the erythroid/megakaryocytic lineage and leads to circulating red cells with a partial deficiency in glycosyl phosphatidylinositol-linked proteins (paroxysmal nocturnal hemoglobinuria type II cells). *Blood* **98**, 2248–2255 (2001).
36. Walkley, C. R., Fero, M. L., Chien, W. M., Purton, L. E. & McArthur, G. A. Negative cell-cycle regulators cooperatively control self-renewal and differentiation of haematopoietic stem cells. *Nature Cell Biol.* **7**, 172–178 (2005).
37. Choi, J. W., Kim, Y., Fujino, M. & Ito, M. A new anti-hemoglobin F antibody against synthetic peptides for the detection of F-cell precursors (F-blasts) in bone marrow. *Int. J. Hematol.* **74**, 277–280 (2001).
38. Bolland, D. J. *et al.* Antisense intergenic transcription in V(D)J recombination. *Nature Immunol.* **5**, 630–637 (2004).

Bioelectromagnetics 30:280 – 285 (2009)

Exposure to a MRI-Type High-Strength Static Magnetic Field Stimulates Megakaryocytic/ Erythroid Hematopoiesis in CD34$^+$ Cells From Human Placental and Umbilical Cord Blood

Satoru Monzen,[1] Kenji Takahashi,[1] Tsutomu Toki,[2] Etsuro Ito,[2] Tomonori Sakurai,[1] Junji Miyakoshi,[1] and Ikuo Kashiwakura[1]*

[1]*Department of Radiological Life Sciences, Division of Medical Life Sciences, Hirosaki University Graduate School of Health Sciences, Hirosaki, Japan*
[2]*Department of Pediatrics, Hirosaki University Graduate School of Medicine, Hirosaki, Japan*

The biological response after exposure to a high-strength static magnetic field (SMF) has recently been widely discussed from the perspective of possible health benefits as well as potential adverse effects. To clarify this issue, CD34 cells from human placental and umbilical cord blood were exposed under conditions of high-strength SMF in vitro. The high-strength SMF exposure system was comprised of a magnetic field generator with a helium-free superconducting magnet with built-in CO_2 incubator. Freshly prepared CD34 cells were exposed to a 5 tesla (T) SMF with the strongest magnetic field gradient (41.7 T/m) or a 10 T SMF without magnetic field gradient for 4 or 16 h. In the harvested cells after exposure to 10 T SMF for 16 h, a significant increase of hematopoietic progenitors in the total burst-forming unit erythroid- and megakaryocytic progenitor cells-derived colony formation was observed, thus producing 1.72- and 1.77-fold higher than the control, respectively. Furthermore, early hematopoiesis-related and cell cycle-related genes were found to be significantly up-regulated by exposure to SMF. These results suggest that the 10 T SMF exposure may change gene expressions and result in the specific enhancement of megakaryocytic/erythroid progenitor (MEP) differentiation from pluripotent hematopoietic stem cells and/or the proliferation of bipotent MEP. Bioelectromagnetics 30:280–285, 2009.

Key words: static magnetic fields; CD34 cells; hematopoietic progenitor cells; megakaryocytic/ erythroid hematopoiesis; MRI

INTRODUCTION

Man-made static magnetic fields (SMF) are used in research and in medical applications such as magnetic resonance imaging (MRI) which provides three-dimensional images of the brain and other soft tissues. Scanned patients and machine operators can therefore be exposed to very high-strength SMF. The biological response after exposure to high-strength SMF has recently been widely discussed from the perspective of possible health benefits as well as potential adverse effects. Currently, stronger SMF up to 9.4 T are used for whole-body scanning to obtain higher resolution imaging in research applications [Sosnovik et al., 2007]. Guidelines for patient exposure to MRI are given by the U.S. Food and Drug Administration, International Electrotechnical Commission, National Radiological Protection Board and International Commission on Non-Ionizing Radiation Protection [Rockville, 1982; IEC 60601-2-33, 2002; Kanal et al., 2002; International Commission on Non-Ionizing Radiation Protection, 2004]. Despite these guidelines and the study of various biological effects induced by a high-strength SMF [Miyakoshi, 2005], there are still important safety issues regarding such exposure. The hematopoietic system is sensitive to extracellular oxidative stresses, such as

Contract grant sponsor: Fund for the promotion of international scientific research (Hirosaki, Aomori).

*Correspondence to: Ikuo Kashiwakura, Department of Radiological Life Sciences, Division of Medical Life Sciences, Hirosaki University Graduate School of Health Sciences, 66-1 Hon-cho, Hirosaki 036-8564, Japan. E-mail: ikashi@cc.hirosaki-u.ac.jp

Received for review 2 July 2008; Final revision received 11 November 2008

DOI: 10.1002/bem.20480
Published online 24 February 2009 in Wiley InterScience (www.interscience.wiley.com).

radiation or chemotherapy [Hamimovitz-Friedman, 1998; Wright, 1998; Schmidt-Ullrich et al., 2000; Nagayama et al., 2002; Kashiwakura et al., 2007]. However, very few studies so far have described the effects of SMF on the proliferation and differentiation of human hematopoietic stem-progenitor cells in comparison to other cellular investigations.

Recently, we designed and manufactured a system for the long-term exposure of cells to high-field-strength SMF [Nakahara et al., 2002]. In the present study, the effects of SMF on the proliferation and differentiation of human hematopoietic stem cells, CD34 cells prepared from human placental and umbilical cord blood (CB), were evaluated.

MATERIALS AND METHODS

Preparation of CB CD34 Cells

The experiments using CB CD34 cells were approved by the Committee of Medical Ethics of Hirosaki University School of Medicine (Hirosaki, Japan) [Kashiwakura et al., 2007]. After obtaining informed consent from the mothers, CB was collected at the maternity facility or Hirosaki National Hospital. The CD34 cells were purified using magnetic cell sorting (CD34 MultiSort Kit, Miltenyi Biotec, Bergisch Gladbach, Germany), and were released from the magnetic particle before SMF exposure. At the end of the procedure, the purity of CD34 cells was shown to be about 90–95% using a fluorescence cell analyzer (Epics XL, Beckman Coulter, Fullerton, CA).

Exposure to High-Strength SMF

The high-strength SMF exposure system was comprised of a magnetic field generator with a helium-free superconducting magnet with buit-in CO_2 incubator, which has previously been described elsewhere [Nakahara et al., 2002; Zhang et al., 2003]. The freshly prepared CD34 cells were suspended in serum-free medium without cytokines to exclude the influence by cytokines, then exposed to a 5 T SMF with the strongest magnetic field gradient (41.7 T/m) or a 10 T SMF without magnetic field gradient at 37 °C in a humidified atmosphere containing 5% CO_2 for 4 or 16 h. The magnetic field distribution was measured using a Gauss Meter HGM-8900 with a TS-3X probe (Toyojiki Industry Co., Niiza, Japan).

Progenitor Cells Analysis

Each hematopoietic progenitor cell was assayed for its clonogenic potential. Colony-forming unit granulocyte-macrophage (CFU-GM), burst-forming unit erythroid (BFU-E), and colony-forming unit granulocyte-erythroid-megakaryocyte-macrophage (CFU-Mix) were evaluated using a methylcellulose culture (Methocult H4230, Stem Cell Technologies, Vancouver, Canada) and colony-forming unit megakaryocyte (CFU-Meg) were assayed using the plasma clot technique [Takahashi et al., 2007]. CFU-GM, BFU-E and CFU-Meg-derived colonies are composed of granulocytes/macrophages, erythrocytes and megakaryocytes, respectively. A mass of granulocyte-erythroid-megakaryocyte-macrophage forms the CFU-Mix-derived colony. Recombinant human cytokines were provided by Biosource™ products (Invitrogen, Carlsbad, CA). The methylcellulose culture contained CB CD34 cells, recombinant human granulocyte colony-stimulating factor (10 ng/ml), granulocyte-macrophage colony-stimulating factor (10 ng/ml), stem cell factor (SCF) (100 ng/ml), interleukin-3 (100 ng/ml) and erythropoietin (4 U/ml). The plasma clot technique used platelet-poor human plasma supplemented with thrombopoietin (50 ng/ml) and SCF. Sham control-treated and SMF-exposed CD34 cells were suspended in 1 ml each semi-solid culture medium, and then transferred onto 24-well culture plates (Falcon, Becton Dickinson Biosciences, Franklin Lakes, NJ) at 0.3 ml/well.

Quantitative Real-Time Polymerase Chain Reaction PCR

Purified total RNAs were quantified using a bioanalyzer (Agilent Technologies, Santa Clara, CA). First strand cDNAs were synthesized by iScript cDNA Synthesis Kit (Bio-Rad Lab, Hercules, CA) according to the manufacturer's instructions. Expression of genes was assessed by real-time RT-PCR. Real-time RT-PCR was performed using iQ SYBR Green Supermix and a Chrome 4 (Bio-Rad Lab) with typical amplification parameters (95 °C for 5 min, followed by 40 cycles of 95 °C for 30 s, 62°C for 30 s, and 72 °C for 30 s). Fold-differences were determined by comparing the ΔCt of each gene on differentiation exposed at 10 T for 16 h to that of sham for 16 h after normalization with GAPDH. The oligonucleotide primer sets used in the real-time RT-PCR were purchased from TAKARA Bio (Otsu, Japan) (Table 1).

RESULTS

In Vitro Hematopoietic Progenitor Cells Analysis

After exposure to SMF at 5 or 10 T for 4 or 16 h, cell viability showed no significant differences between the unexposed and exposed CD34 cells (data not shown). In the harvested cells after a 10 T SMF exposure for 16 h, a significant increase in the number of total

TABLE 1. Origins, National Center for Biotechnology Information Gene Accession Numbers and Sequences of Synthetic Oligonucleotide PCR Primers

Gene	Accession number	Primer sequence
GATA1	NM_002049	F: 5′-TGATTGTCAGTAAACGGGCAGGTA-3′ R: 5′-AGTAGAGGCCGCAGGCATTG-3′
GATA2	NM_032638	F: 5′-GGTCCAGCTTTACTGTGGCTGTC-3′ R: 5′-TGGTCACTACATCAGCACAATCCTC-3′
GATA3	NM_001002295	F: 5′-GCAGGAGCAGTATCATGAAGCCTAA-3′ R: 5′-TTGGAACACAGACACCACAGTGAG-3′
RUNX1	NM_001754	F: 5′-TCCCTGGTACAAACGTATGGAATG-3′ R: 5′-GACTGTGTACCGTGGACTGTGGA-3′
c-KIT	NM_000222	F: 5′-TTCCCAAGCCCATGAGTCCT-3′ R: 5′-ACACGTGGAACACCAACATCCT-3′
PCNA	NM_002592	F: 5′-TCTTCAACGGTGACACTCAGTATG-3′ R: 5′-TCGATCTTGGGAGCCAAGTAGTA-3′
CDC25B	NM_021873	F: 5′-CAGTGCCTTGCATACCCAAAC-3′ R: 5′-TTGTCCACACAAATAGGCACACATA-3′
ERN1	NM_001433	F: 5′-TCAGAGACAGCGCGAGTAGCA-3′ R: 5′-TAGCTGTCCCAGCACGCAAG-3′
TAO kinase3	NM_016281	F: 5′-CAAGCGTTACGGCTAGATGAGG-3′ R: 5′-CTCTAGCTTCTGGAGCTCACGTTC-3′
TAL1	NM_003189	F: 5′-ACTTGTGATTTCGATGGTACGTGA-3′ R: 5′-GCCTCTGGGCTGTACAAAGGTC-3′
TEL (ETV6)	NM_001987	F: 5′-TGATGGAAGCAGGCGAGCTA-3′ R: 5′-TGCTCGGTGGCTTGTCTAAGG-3′
PAX5	NM_016734	F: 5′-GAACAGCCAGGTAGAGCCCTTG-3′ R: 5′-CTGCCATCCTGGTGACATACAGA-3′
PU.1	NM_001080547	F: 5′-TCCAGTTCTCGTCCAAGCACA-3′ R: 5′-ACTTCGCCGCTGAACTGGTAG-3′
GAPDH	NM_002046	F: 5′-GCACCGTCAAGGCTGAGAAC-3′ R: 5′-ATGGTGGTGAAGACGCCAGT-3′

The human oligonucleotide primer sets are purchased from Takara Bio.
[a]F, forward primer; R, reverse primer.

CFU-Meg- and BFU-E-derived colony formation was observed, producing 1.72- and 1.77-fold more colonies than the sham control, respectively (Fig. 1). In contrast, the number of CFU-GM and CFU-Mix was not affected, and the 10 T exposure for 4 h or the 5 T SMF resulted in no effect regarding the clonogenicity of each progenitor.

Gene Expression Analysis

To observe this phenomena more precisely, the gene expression of cells exposed to a 10 T SMF for 16 h was examined using real-time RT-PCR. As shown in Figure 2, early hematopoiesis-related genes, such as c-KIT, GATA2, RUNX1 and TEL (1.15-, 1.56-, 1.33-, and 1.45-fold higher level of expression in comparison to the sham control), and cell cycle-related genes, such as CDC25B and ERN1 (1.42- and 1.39-fold higher level of expression in comparison to the sham control), were found to be significantly higher in the cells exposed to a 10 T SMF for 16 h in comparison to the sham control. On the other hand, the other hematopoiesis and/or cell cycle genes analyzed in this study, such as TAL1, GATA1, PU.1, GATA3, PAX5, PCNA, and TAO kinase 3 demonstrated no significant change.

DISCUSSION

In order to clarify the biological response of human hematopoietic stem-progenitor cells after exposure to high-strength SMF, CD34 cells prepared from human CB were exposed under conditions of 10 T SMF without any cytokine stimulation in vitro. The exposed CD34 cells to SMF at 10 T for 16 h resulted in a significant increase in the total CFU-Meg- and BFU-E-derived colony formation in comparison to the sham control (Fig. 1). Onodera et al. [2003] demonstrated that 10 T SMF exposure for 3 h resulted in no significant differences in the viability of CD4 T cells, CD8 T cells, B cells, or natural killer cells prepared from human peripheral blood. Another previous study also showed that long-term exposure to 10 T SMF for up to 4 days did not affect the growth rate or cycle distribution of CHO-K1 cells [Nakahara et al., 2002]. Considering previous studies, these results indicate that exposure to SMF alone has little or an extremely small effect on cell

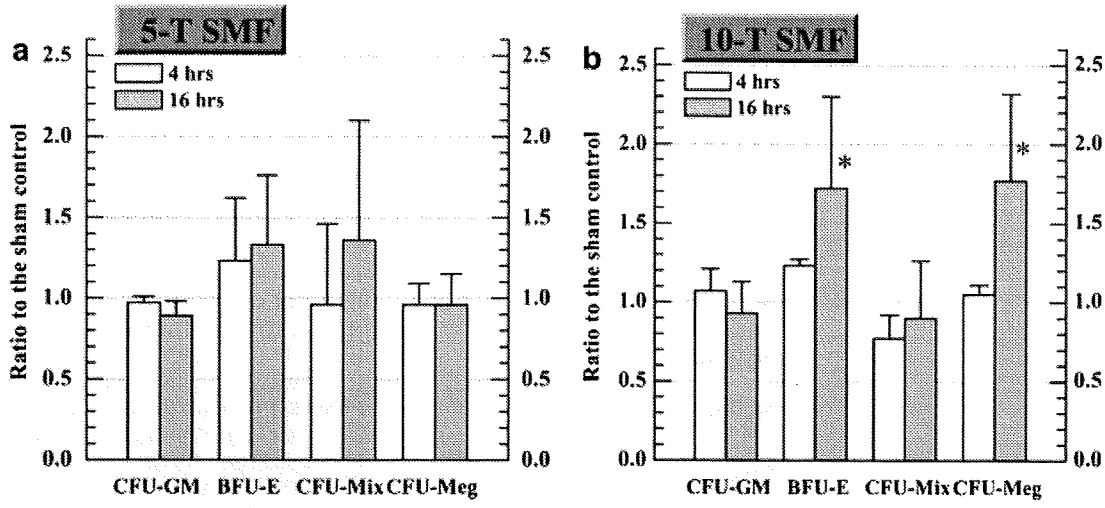

Fig. 1. Effects of exposure to SMF on colony-forming cells. Human CB CD34 cells were exposed to a 5 T (a) or 10 T (b) high-strength SMF exposure at 37 °C in a humidified atmosphere containing 5% CO_2. After exposure for 4 or 16 h, the cells were harvested, assayed for hematopoietic progenitor cells in semi-solid culture with cytokines and incubated for 11–14 days. The values are the mean ± SD of more than three separate experiments in three wells. $^*P < 0.05$.

growth and genetic toxicity regardless of the magnetic density. Therefore, the present results obtained using CD34 cells prepared from CB demonstrate a remarkable effect of SMF.

An analysis of genes expression showed that c-KIT, GATA2, RUNX1, TEL, CDC25B, and ERN1 were significantly higher in cells exposed to 10 T SMF for 16 h. Among the genes upregulated here, GATA2, RUNX1, and TEL are known to be involved as early hematopoiesis-related transcription factors [Wiemels et al., 1999]. In addition, all these genes have demonstrated the implications of megakaryocytic and erythroid differentiation in cell lines [Escribano et al., 1998; Ikonomi et al., 2000; Takahashi et al., 2005; Lulli et al., 2006; Nagai et al., 2006]. Among the other upregulated genes, CDC25B is a member of the CDC25 family of phosphatases that activates the cyclin-dependent kinase CDC2 by removing two phosphate groups and it is required for entry into mitosis [Kieffer et al., 2007]. In addition, the ERN-encoded protein possesses an intrinsic kinase activity and an endoribonuclease activity, which play an important role in altering the gene expression as a response to endoplasmic reticulum-based stress signals [Tirasophon et al., 1998]. Although it is unclear precisely how high-strength SMF acts on these genes, and regulates the proliferation and differentiation of hematopoietic stem/progenitor cells, the present study firstly presents evidence that SMF specifically stimulates megakaryocytic/erythroid hematopoiesis and up-regulates its related genes expression. On the other hand, the other genes analyzed in this study, such as TAL1, GATA1, PU.1, GATA3, PAX5, PCNA, and TAO kinase 3 demonstrated no significant change. Within the definitive hematopoietic hierarchy, TAL1 is expressed in hematopoietic stem cells and multipotent progenitors, as well as cells of the erythroid, megakaryocytic, and mastocytic lineages [Elwood et al., 1998; Lécuyer and Hoang, 2004; Zhang et al., 2005; Brunet de la Grange et al., 2006]. Therefore, almost no responded genes are related to lineage-committed stem/progenitor cells or terminal differentiation pathways in hematopoiesis.

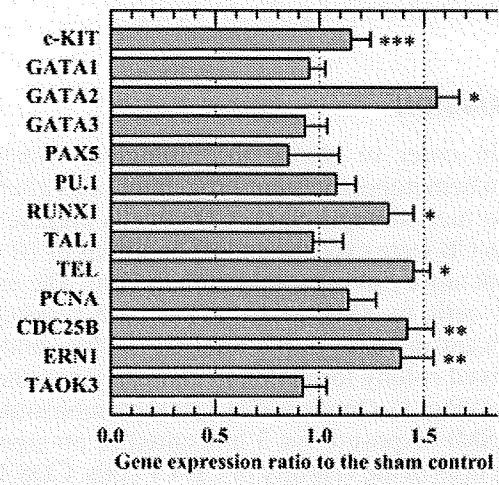

Fig. 2. Gene expression of hematopoietic stem cells after exposure to high-strength SMF. Total RNA were extracted from CB CD34 cells after exposure to 10 T for 16 h. The quantification of gene expression was analyzed using the real-time RT-PCR method. Gene expression was calculated using a "Gene Expression Analysis for iCycler iQ Real-time PCR Description System". The values are the mean ± SD of four separate experiments. $^*P < 0.001$, $^{**}P < 0.01$, $^{***}P < 0.05$.

Thus, SMF may have a potential to regulate the early stage of hematopoiesis from multipotent hematopoietic stem cells to committed progenitor cells, especially MEP (Fig. 3). Considering the information described above, we are now planning to carry out further investigations in order to more precisely determine these mechanisms.

A human study based on a pregnant MRI worker [Kanal et al., 1993] surveyed female technicians in the USA to establish the effects of exposure to static field fringe fields on pregnant staff. A white paper [Kanal et al., 2002] advises pregnant Health Care Practitioners that pregnant health care workers are permitted to work in and around the MRI environment throughout all stages of pregnancy. MRI is useful for assessing the functionality and condition of the placenta, amniotic fluid, etc. [De Wilde et al., 2005]. However, the international standard (IEC 60601-2-33) [IEC 60601-2-33, 2002], expresses caution for imaging pregnant women and states that there is no conclusive evidence to establish safety. Current recommendations in the UK say that it is advisable not to scan in the first trimester [Medical Devices Agency, 2002]. In addition, De Wilde et al. [2005] recommends performing risk assessment for pregnant staff working in MRI, and advises that there is a clear need for further research into the effects of MRI in pregnancy to provider clear, authoritative advice. Recently, Saito et al. [2006] reported that high dose SMF at 400 mT for 1 h from a constant direction on a selected day of pregnancy between GD 7.5 and 14.5 caused malformations in mouse fetuses. All up-regulated genes observed in the present study are associated with a specific type of oncogenesis. Feychting [2005] reported that the available evidence from epidemiological studies is not yet sufficient to draw any conclusions about the potential health effects of static magnetic field exposure. In the age when an increasing exposure to static magnetic fields is occurring in the general public, she worries that there is no scientific basis for the assumption that such exposure has no long-term health effects. In conclusion, we should therefore pay attention to carefully balance the risks, in particular to embryos, and the benefits that can be obtained when using the technical innovation of SMF.

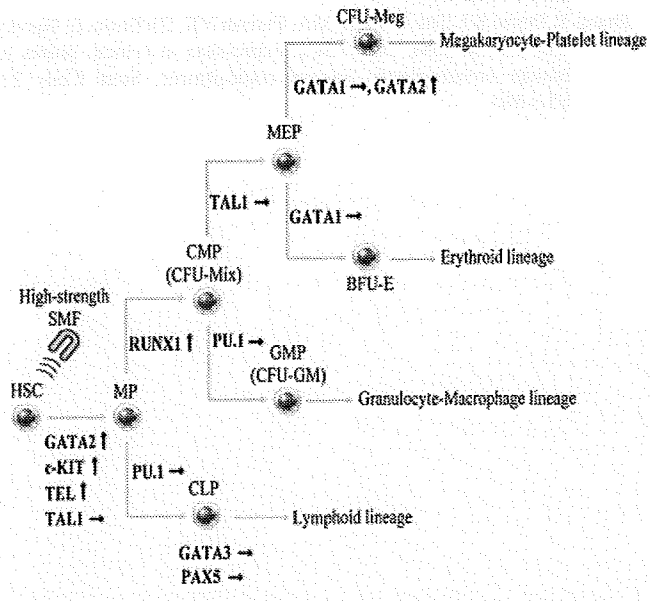

Fig. 3. A functional distribution of analyzed genes and its changing by static magnetic exposure in Hematopoietic differentiation. The upper arrows bar "↑" means significant up-regulation in comparison to the sham control, and the right arrows bar "→" means no significant changing. CLP, common lymphoid progenitors; CMP, common myeloid progenitors; GMP, granulocyte macrophage progenitors.

ACKNOWLEDGMENTS

This study was supported by the fund for the promotion of international scientific research (Hirosaki, Aomori). We thank the Fukushi maternity facility located in Goshogawara-shi (Aomori, Japan) and Hirosaki National Hospital (Aomori, Japan) where the CB was collected for this study.

REFERENCES

Brunet de la Grange P, Armstrong F, Duval V, Rouyez MC, Goardon N, Romeo PH, Pflumio F. 2006. Low SCL/TAL1 expression reveals its major role in adult hematopoietic myeloid progenitors and stem cells. Blood 108:2998–3004.

De Wilde JP, Rivers AW, Price DL. 2005. A review of the current use of magnetic resonance imaging in pregnancy and safety implications for the fetus. Prog Biophys Mol Biol 87:335–353.

Elwood NJ, Zogos H, Pereira DS, Dick JE, Begley CG. 1998. Enhanced megakaryocyte and erythroid development from normal human CD34() cells: Consequence of enforced expression of SCL. Blood 91:3756–3765.

Escribano L, Ocqueteau M, Almeida J, Orfao A, San Miguel JF. 1998. Expression of the c-kit (CD117) molecule in normal and malignant hematopoiesis. Leuk Lymphoma 30:459–466.

Feychting M. 2005. Health effects of static magnetic fields: A review of the epidemiological evidence. Prog Biophys Mol Bio 87: 241–246.

Hamimovitz-Friedman A. 1998. Radiation-induced signal transduction and stress response. Radiat Res 150:S102–S108.

ICNIRP. 2004. International Commission on Non-Ionizing Radiation Protection. Medical MR procedures, protection of patient, volunteer and staff. Health Phys. 2004. 87:197–216.

IEC 60601-2-33. 2002. Particular Requirements for the Safety of Magnetic Resonance Equipment for Medical Diagnosis. International Electrical Comission, Geneva, Switzerland.

Ikonomi P, Rivera CE, Riordan M, Washington G, Schechter AN, Noguchi CT. 2000. Overexpression of GATA-2 inhibits erythroid and promotes megakaryocyte differentiation. Exp Hematol 28:1423–1431.

Kanal E, Gillen J, Evans JA, Savitz DA, Shellock FG. 1993. Survey on reproductive health among female MR workers. Radiology 187:395–399.

Kanal E, Borgstede JP, Barkovich AJ, Bell C, Bradley WG, Felmlee JP, Froelich JW, Kaminski EM, Keeler EK, Lester JW, Scoumis EA, Zaremba LA, Zinninger MD. American College of Radiology. 2002. American College of Radiology white paper on MR safety. Am J Radiol 178:1335–1347.

Kashiwakura I, Takahashi K, Takagaki K. 2007. Application of proteoglycan extracted from the nasal cartilage of salmon heads for ex vivo expansion of hematopoietic progenitor cells derived from human umbilical cord blood. Glycoconj J 24:251–258.

Kieffer I, Lorenzo C, Dozier C, Schmitt E, Ducommun B. 2007. Differential mitotic degradation of the CDC25B phosphatase variants. Oncogene 26:7847–7858.

Lécuyer E, Hoang T. 2004. SCL: From the origin of hematopoiesis to stem cells and leukemia. Exp Hematol 32:11–24.

Lulli V, Romania P, Morsilli O, Gabbianelli M, Pagliuca A, Mazzeo S, Testa U, Peschle C, Marziali G. 2006. Overexpression of Ets-1 in human hematopoietic progenitor cells blocks erythroid and promotes megakaryocytic differentiation. Cell Death Differ 13:1064–1074.

Medical Devices Agency. 2002. Guidelines for Magnetic Resonance Diagnostic Equipment in Clinical Use. Medicines and Healthcare products Regulatory Agency, London.

Miyakoshi J. 2005. Effects of static magnetic fields at the cellular level. Prog Biophys Mol Biol 87:213–223.

Nagai R, Matsuura E, Hoshika Y, Nakata E, Nagura H, Watanabe A, Komatsu N, Okada Y, Doi T. 2006. RUNX1 suppression induces megakaryocytic differentiation of UT-7/GM cells. Biochem Biophys Res Commun 345:78–84.

Nagayama H, Misawa K, Tanaka H, Ooi J, Iseki T, Tojo A, Tani K, Yamada Y, Kodo H, Takahashi TA, Yamashita N, Shimazaki S, Asano S. 2002. Transient hematopoietic stem cell rescue using umbilical cord blood for a lethally irradiated nuclear accident victim. Bone Marrow Transplant 29:197–204.

Nakahara T, Yaguchi H, Yoshida M, Miyakoshi J. 2002. Effects of exposure of CHO-K1 cells to a 10 T static magnetic field. Radiology 224:817–822.

Onodera H, Jin Z, Chida S, Suzuki Y, Tago H, Itoyama Y. 2003. Effects of 10 T static magnetic field on human peripheral blood immune cells. Radiat Res 159:775–779.

Saito K, Suzuki H, Suzuki K. 2006. Teratogenic effects of static magnetic field on mouse fetuses. Reprod Toxicol 22:118–124.

Schmidt-Ullrich RK, Dent P, Grant S, Mikkelsen RB, Valerie K. 2000. Signal transduction and cellular radiation responses. Radiat Res 153:245–257.

Sosnovik DE, Dai G, Nahrendorf M, Rosen BR, Seethamraju R. 2007. Cardiac MRI in mice at 9.4 Tesla with a transmit-receive surface coil and a cardiac-tailored intensity-correction algorithm. J Magn Reson Imaging 26:279–287.

Takahashi W, Sasaki K, Komatsu N, Mitani K. 2005. TEL/ETV6 accelerates erythroid differentiation and inhibits megakaryocytic maturation in a human leukemia cell line UT-7/GM. Cancer Sci 96:340–348.

Takahashi K, Monzen S, Eguchi-Kasai K, Abe Y, Kashiwakura I. 2007. Severe damage of human megakaryocytopoiesis and thrombopoiesis by heavy-ion beam radiation. Radiat Res 168: 545–551.

Tirasophon W, Welihinda AA, Kaufman RJ. 1998. A stress response pathway from the endoplasmic reticulum to the nucleus requires a novel bifunctional protein kinase/endoribonuclease (Ire1p) in mammalian cells. Genes Dev 12:1812–1824.

U.S. Radiological Health Bureau. 1982. Guidelines for evaluating electromagnetic exposure risk for trials of clinical NMR systems. Rockville, MD: U.S. Food and Drug Administration.

Wiemels JL, Cazzaniga G, Daniotti M, Eden OB, Addison GM, Masera G, Saha V, Biondi A, Greaves MF. 1999. Prenatal origin of acute lymphoblastic leukaemia in children. Lancet 354: 1499–1503.

Wright EG. 1998. Radiation-induced genomic instability in haemopoietic cells. Int J Radiat Biol 74:681–687.

Zhang QM, Tokiwa M, Doi T, Nakahara T, Chang PW, Nakamura N, Hori M, Miyakoshi J, Yonei S. 2003. Strong static magnetic field and the induction of mutations through elevated production of reactive oxygen species in Escherichia coli soxR. Int J Radiat Biol 79:281–286.

Zhang Y, Payne KJ, Zhu Y, Price MA, Parrish YK, Zielinska E, Barsky LW, Crooks GM. 2005. SCL expression at critical points in human hematopoietic lineage commitment. Stem Cells 23: 852–860.

Tohoku J. Exp. Med., 2009, 217, 223-229

Bach1 Deficiency Ameliorates Hepatic Injury in a Mouse Model

Akio Iida,[1] Koji Inagaki,[1] Akira Miyazaki,[1] Fumihiko Yonemori,[1] Etsuro Ito[2] and Kazuhiko Igarashi[3]

[1]Japan Tobacco Inc., Central Pharmaceutical Research Institute, Osaka, Japan
[2]Department of Pediatrics, Hirosaki University School of Medicine, Hirosaki, Aomori, Japan
[3]Department of Biochemistry, Tohoku University Graduate School of Medicine, Sendai Japan

Bach1 is a basic region-leucine zipper (bZip) protein that forms heterodimers with the small Maf proteins and functions as a repressor of gene expression. One of the target genes of Bach1 is *Hmox-1* that encodes heme oxygenase-1 (HO-1). HO-1 degrades heme into carbon monoxide (CO), biliverdin, and iron. HO-1 is strongly induced by various stresses as well as its substrate heme, and protects cells and tissues against insults through diverse cytoprotective functions of the reaction products CO and biliverdin. *Bach1*-deficiency in mice leads to higher expression of *Hmox-1* in various tissues. Here we investigated the effects of *Bach1*-deficiency in mice on tissue injuries: hepatic injury induced by D-galactosamine (GalN) and lipopolysaccharide (LPS), and mouse paw edema induced by carrageenin, polysaccharide derived from various seaweeds. *Bach1*-deficiency suppressed induction of plasma alanine aminotransferase (ALT) and aspartate aminotransferase (AST) activities in response to the GalN/LPS-treatment. However, production of tumor necrosis factor alpha (TNF-α) and nitric oxide (NO), both being cytotoxic mediators in LPS-induced hepatic injury, in *Bach1*-deficient mice and their peritoneal macrophages was similar to wild type controls. In contrast, *Bach1*-deficiency did not affect extent of mouse paw edema induced by carrageenin, which enhances vascular permeability by activating kinin release. These results indicate that Bach1 plays an inhibitory role in the cytoprotection of LPS-induced liver injury but not in the kinin-mediated inflammatory edema. The inhibitory role for Bach1 may stem from its activity to repress gene expression including HO-1.

——— transcription factor; oxidative stress; heme oxygenase; Maf; liver.
Tohoku J. Exp. Med., 2009, 217 (3), 223-229.

Bach1 is a basic region-leucine zipper (bZip) transcription factor that forms heterodimers with the small Maf proteins. The resulting Bach1 heterodimers bind to the Maf recognition elements (MAREs) to repress transcription (Oyake et al. 1996; Igarashi et al. 1998; Ogawa et al. 2001; Sun et al. 2002; Sun et al. 2004). Other bZip transcription factors such as NF-E2 related factor (Nrf)1 and Nrf2, distantly related to Bach1 (Amoutzias et al. 2007), also form heterodimers with the small Maf proteins, bind to MARE, and activate transcription. As such, MARE-dependent transcription is finely tuned by both repressors and activators (Motohashi et al. 2002; Igarashi and Sun 2006). The balance of repression and activation is modulated in part by heme: direct binding of heme to Bach1 inhibits the DNA binding activity of Bach1/small Maf heterodimer and induces nuclear export of Bach1 (Ogawa et al. 2001; Sun et al. 2002; Suzuki et al. 2004). Furthermore, heme induces polyubiquitination and subsequent degradation of Bach1 (Zenke-Kawasaki et al. 2007). MARE or MARE-like sequences are present in regulatory regions of various genes that are related to heme, oxidative stress response, and xenobiotics metabolism (Kyo et al. 2004). One of the well characterized target genes of Bach1 is *Hmox-1* that encodes heme oxygenase-1 (HO-1). Expression of *Hmox-1* in cultured cells or in organs is very low under normal conditions due to Bach1-mediated repression but is highly induced by its substrate heme, oxidative stress, or other diverse stimuli such as cytokines, heavy metals and heat shock (Shibahara et al. 1985, 1987; Alam et al. 1989; Keyse and Tyrrell 1989; Taketani et al. 1989). *Hmox-1* is constitutively expressed at higher levels in many tissues of *Bach1*-deficient mice, indicating that Bach1 acts as a negative regulator of transcription of *Hmox-1* (Sun et al. 2002; Omura et al. 2005).

HO-1 catalyzes oxidative degradation of heme, generating iron, carbon monoxide, and biliverdin, which is rapidly reduced to bilirubin. Carbon monoxide, biliverdin, and bilirubin possess antioxidant and anti-inflammatory actions (Baranano et al. 2002; Otterbein et al. 2003). Consistent with their protective actions, induction of HO-1 under diverse stress conditions have been shown to protect cells and tissues. For example, HO-1 protects cultured fibroblasts and endothelial cells from TNF-induced apoptosis

Received November 25, 2008; revision accepted for publication February 12, 2009.
Correspondence: Kazuhiko Igarashi, Department of Biochemistry, Tohoku University Graduate School of Medicine, Sendai 980-8575, Japan.
e-mail: igarak@m.tains.tohoku.ac.jp

(Brouard et al. 2000; Petrache et al. 2000). In addition, HO-1 induction confers protective action in various models of organ injuries *in vivo* (Alam et al. 1989; Choi and Alam 1996; Yang et al. 1999; Chen et al. 2000; Shimizu et al. 2000; Akagi et al. 2002; Nakahira et al. 2003; Sass et al. 2003; Dorman et al. 2004). Conversely, the physiological importance of HO-1 encoded by *Hmox1* gene has been shown by the phenotypic consequences of the *Hmox1*-deficient mice that show a hypersensitivity to the oxidative damage and cytotoxicity caused by hemin and hydrogen peroxide (Poss and Tonegawa 1997a, 1997b) and by a patient with *HMOX1*-deficiency (Yachie et al. 1999). Therefore, there is a possibility that Bach1 is an inhibitory factor of cell and tissue defense systems as a repressor of *Hmox-1* and/or other genes. Consistent with this idea, genetic ablation of Bach1 in mice results in reduction of tissue damage after ischemic-reperfusion injury of heart (Yano et al. 2006) and reduction of arteriosclerosis after cuff injury (Omura et al. 2005).

To further understand the function of Bach1 in protective responses against various stresses, we examined the effects of *Bach1* deficiency on galactosamine (GalN)/lipopolysaccharide (LPS)-induced liver injury, which is known to be alleviated by induction of HO-1 (Sass et al. 2003). It was reported previously that LPS-induced hepatic injury is caused by hepatocyte apoptosis mediated by tumor necrosis factor alpha (TNF-α) and nitric oxide (NO) (Lehmann et al. 1987; Morikawa et al. 1999; Sass et al. 2003; Wolf et al. 2005). Thus, we compared LPS-induced TNF-α and NO production in *Bach1*-deficient and control mice. Because HO-1 suppresses inflammatory response to carrageenin (Willis et al. 1996), we also examined the effect of *Bach1*-deficiency in carrageenin-induced mouse paw edema as an inflammation model.

Materials and Methods

Reagents

Galactosamine (GalN) was from Wako Pure Chemical Industries, Ltd. (Osaka, Japan). Lipopolysaccharide (LPS) was from Sigma (St Louis, MO). Hyperfilm ECL and ECL plus detection reagent were from Amersham Biosciences, Inc. (Buckinghamshire, England). Horseradish peroxidase-coupled goat anti-rabbit IgG was from Kirkegaard & Perry Laboratories, Inc. (Gaithersburg, Maryland). λ-Carrageenin (Picnin A) was from Zushikagaku Laboratory (Kanagawa, Japan).

Animals

Generation of *Bach1*$^{-/-}$ mice on a C57BL/6J background has been reported elsewhere (Sun et al. 2002). *Bach1*$^{+/+}$, *Bach1*$^{+/-}$ and *Bach1*$^{-/-}$ mice aged 7–12 weeks were kept on a 12-h light / dark cycle with free access to food and sterile water. All the experiments received prior approval from the committee for the human care and use of animals of our laboratory (Japan Tobacco Inc., Central Pharmaceutical Research Institute), in accordance with the Standards Relating to the Care and Management of Experimental Animals (Notification No. 6, March 27, 1980, of the Prime Minister's Office of Japan).

GalN/LPS-induced liver injury model

Mice were injected intraperitoneally (i.p.) with GalN (500 mg/kg) and LPS (3 μg/kg). Heparinized blood was obtained from the orbital sinus of the mice at 1 and 6 hours after GalN/LPS injection. Blood plasma was separated from heparinized whole blood by centrifugation at 2000 × *g* for 3 minutes at 4°C. The activities of plasma ALT and AST at 6 hours after GalN/LPS injection, the marker enzymes of liver injury, were measured with Monarch (Instrumentation Laboratory, Lexington MA). Plasma concentration of TNF-α at 1 hour after GalN/LPS injection was measured with commercial murine TNF-α ELISA kit (Quantikine M; R&D Systems, Mineapolis, MN).

Macrophage culture and LPS stimulation

Resident macrophages were obtained from the mice by lavage of the peritoneal cavity with 5 ml of sterile phosphate buffer solution containing 10 U/ml heparin. Cells were washed three times with RPMI 1640 containing 10% fetal bovine serum at 4°C . The macrophages at 2 × 10^6 cells/ml were incubated in RPMI 1640 medium in 450 μl/well in a 24-well tissue culture plate. Macrophages were stimulated with LPS solution (final concentration; 1 μg/ml). All cell cultures were maintained at 37°C in a humidified incubator containing 5% CO_2 in air. The results of preliminary investigations showed that secretion of TNF-α and NO from macrophages stimulated by LPS became saturated after 12–24 hours (data not shown). Therefore, culture fluids were collected at 19 hours after incubation. TNF-α concentration of culture supernatants were measured with commercial murine TNF-α ELISA kit. NO was measured as its end product, nitrite, by using Griess reagent as described previously (Wang et al. 1994). The supernatant (10 μl) diluted with phosphate buffer solution (40 μl). The diluted supernatant was mixed with 50 μl of Griess reagent for 10 minutes, and the absorbance at 570 nm was measured in a microplate reader. The concentration of nitrite in the samples was determined with reference to a sodium nitrite standard curve. The data represents the mean of triplicate determinations ± SEM. The adherent cells were lysed on ice with lysis buffer composed of 50 mmol/L Tris/HCl (pH 6.8), 10% glycerol and 1% SDS at 4°C for 30 minutes. These lysis samples were assessed with western blot analysis described below.

Western Blot Analysis

Insoluble materials in the lysis samples described above were removed by centrifugation at 15,000 × g at 4°C for 10 minutes. The supernatants (1 mg protein/ml) were boiled in SDS-PAGE sample buffer for 3 minutes. After a brief centrifugation, the supernatants (20 μl/lane) were separated by SDS-PAGE and then electroblotted onto nitrocellulose membrane. The blots were blocked with 3% skim milk in PBS at room temperature for 1 hour and then incubated with primary anti-HO-1 antibody (Stressgen) at 1 : 2000 at room temperature for 1 hour. After washing with PBS containing 0.1% Tween 20, the blots were probed with secondary antibody (horseradish peroxidase-coupled goat anti-rabbit IgG at 1 : 5000) at room temperature for 1 hour. After a second wash, the blots were exposed to Hyperfilm ECL and ECL plus detection reagent to enable visualization of phosphotyrosine-containing proteins.

Carrageenin-Induced Paw Edema

Right hind paw of mouse was measured by plethysmometer (TK-101; Unicom Inc., Chiba, Japan) 2 h before Carrageenin inoculation. Carrageenin was dissolved in saline by incubation for 24 h at

4°C to make up 1% solution and inoculated subcutaneously at a volume of 50 μl at foot pad of the right hind paw. At 2, 3, 5, 24 hours after carrageenin injection, paw volume was measured and compared with predosing value, and the edema formation of each mouse was determined. All the measurements were performed in a blind manner. Data were calculated as percentage of increase of the paw volume by comparing pre- and post-carrageenin injection.

Statistical analysis

Data are expressed as mean ± SEM. The statistical significance was determined by Student's *t* test or Aspin-welch *t* test.

Results

Effects of Bach1-deficiency on GalN/LPS-induced liver injury

Combined injection of GalN and LPS causes massive liver injury due to apoptotic cell death (Morikawa et al. 1996). We compared the effects of *Bach1*-deficiency on GalN/LPS-induced liver injury using *Bach1*$^{+/+}$, *Bach1*$^{+/-}$ and *Bach1*$^{-/-}$ mice. Injection of GalN/LPS significantly increased plasma ALT and AST activities in *Bach1*$^{+/+}$ mice that reflected liver injury (Fig. 1A and B). Release of ALT and AST activities after GalN/LPS treatment was significantly suppressed in *Bach1*$^{-/-}$ mice. Interestingly, it was also reduced to some extent in *Bach1*$^{+/-}$ mice. Considering that LPS-induced cytotoxicity is mainly mediated by TNF-α (Lehman et al. 1987; Tiegs et al. 1989; Morikawa et al. 1996), we next examined plasma levels of TNF-α (Fig. 1C). While the level of TNF-α in wild-type mice sera was 60-70 pg/ml without any treatment, it increased at 1 hour after GalN/LPS injection and then returned to basal level by 6 hours (data not shown). Plasma concentration of TNF-α in *Bach1*$^{-/-}$ mice similarly increased after injection of GalN/LPS. No significant change in viability of mice was observed.

Bach1-deficiency does not affect LPS-induced TNF-α and NO production in macrophages

Macrophages produce proinflammatory cytokines including TNF-α and IL-6 in response to LPS. To investi-

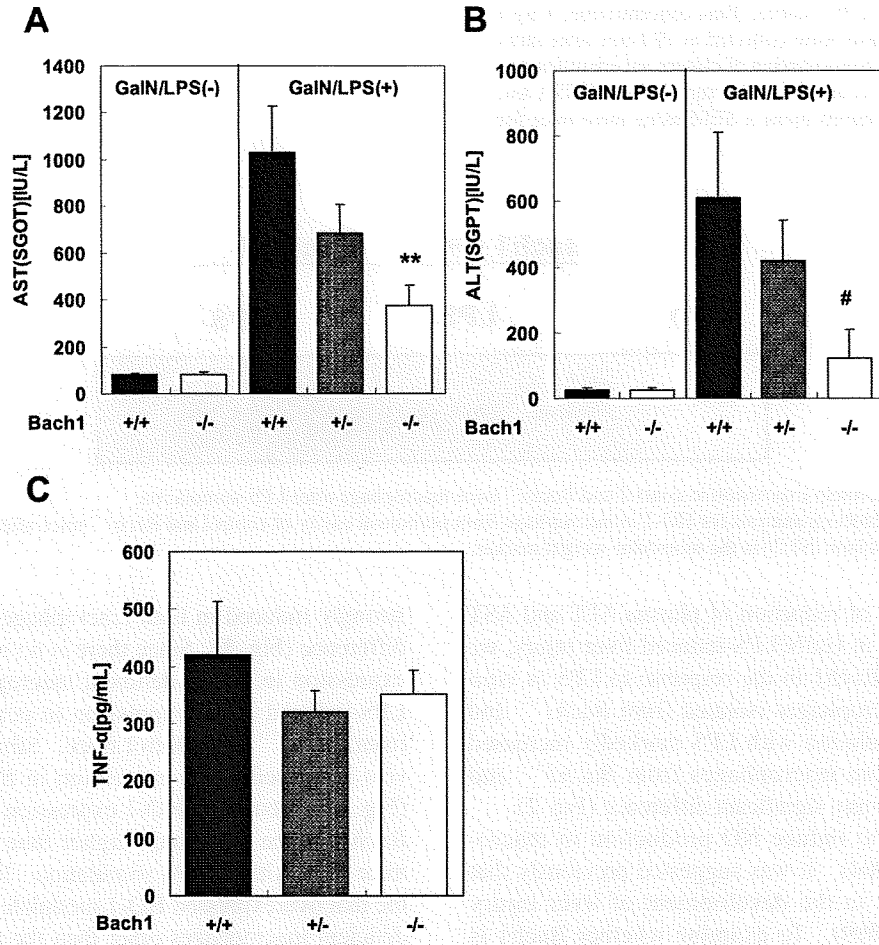

Fig. 1. Effects of GalN/LPS injection on plasma AST, ALT and TNF-α levels in control and *Bach1*$^{-/-}$ mice.
(A and B) The activities of plasma aminotransferase (ALT and AST) at 6 hours after GalN/LPS injection. Each value represents mean ± SEM ([GalN/LPS(-)] *Bach1*$^{+/+}$, $n = 8$; *Bach1*$^{-/-}$, $n = 9$; [GalN/LPS(+)] *Bach1*$^{+/+}$, $n = 5$; *Bach1*$^{+/-}$, $n = 5$; *Bach1*$^{-/-}$, $n = 6$). (C) Plasma concentration of TNF-α at 1 hour after GalN/LPS injection. Each value represents mean ± SEM (*Bach1*$^{+/+}$, $n = 5$; *Bach1*$^{+/-}$, $n = 5$; *Bach1*$^{-/-}$, $n = 6$). Statistical analysis was performed by Student's *t* test (**, $p < 0.01$) or by Aspin-welch *t* test (#, $p < 0.05$) v.s. control mice.

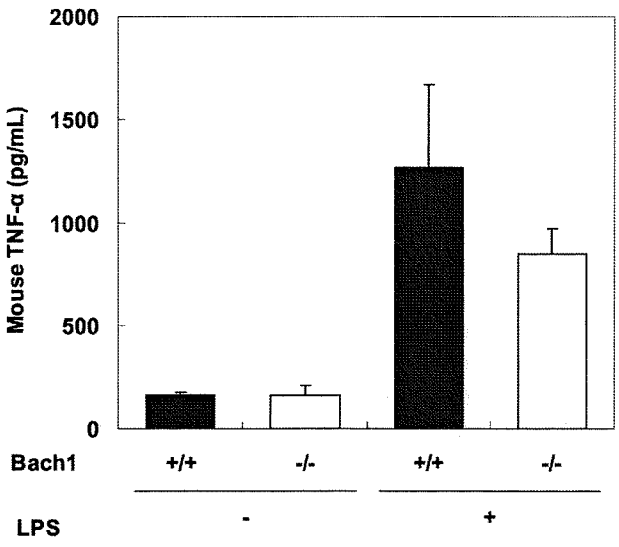

Fig. 2. TNF-α production of LPS-stimulated macrophage from peritoneal cavity in control and *Bach1*$^{-/-}$ mice.
Resident macrophages were obtained from the mice by lavage of the peritoneal cavity. Both macrophages were stimulated with LPS solution (final concentration; 1 μg/1 ml). Culture fluids were collected at 19 hours after incubation. TNF-α concentration of culture supernatants was measured with commercial murine TNF-α ELISA kit. Each value represents mean ± SEM using three mice for each group.

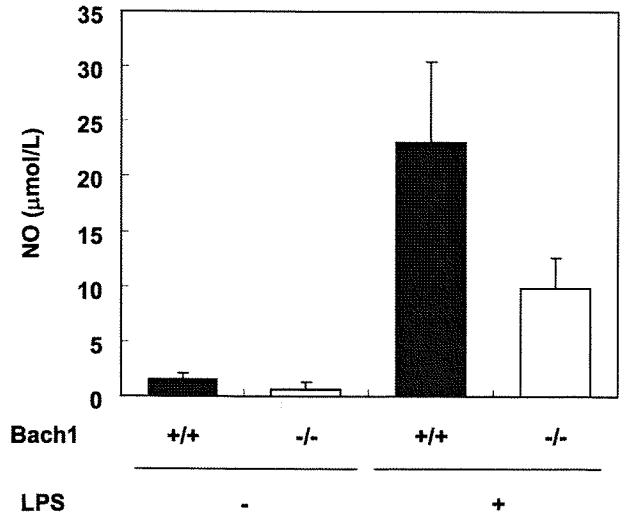

Fig. 3. NO production of LPS-stimulated macrophage in control and *Bach1*$^{-/-}$ mice.
Macrophages were stimulated with LPS as in Fig. 2. NO was measured as its end product, nitrite, by using Griess reagent. Each value represents mean ± SEM using three mice for each group.

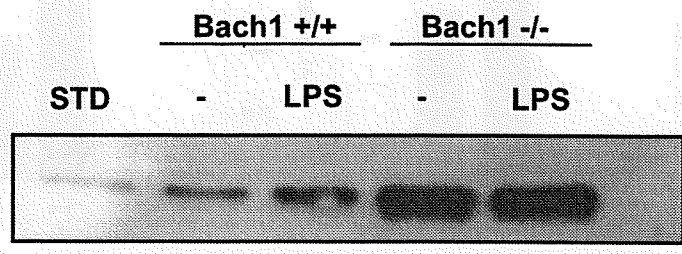

Fig. 4. HO-1 protein expression in control and *Bach1*$^{-/-}$ mice macrophage after LPS-stimulation.
Western blotting analysis for HO-1 in macrophage from peritoneal cavity of control and *Bach1*$^{-/-}$ mice after LPS-stimulation. Left lane (STD) is the molecular-weight marker.

gate the mechanisms of reduction of plasma ALT and AST by *Bach1*-deficiency in GalN/LPS-induced liver injury, we assessed the role of Bach1 in the response to LPS *in vitro* using peritoneal macrophages isolated from *Bach1*$^{+/+}$ and *Bach1*$^{-/-}$ mice. Stimulation with LPS markedly increased TNF-α secretion from macrophages from *Bach1*$^{+/+}$ and *Bach1*$^{-/-}$ mice without any significant difference (Fig. 2).

LPS is known to induce NO production in macrophages (Lee et al. 2004). It was suggested previously that NO may participate in the development of liver injury (Morikawa et al. 1999). To examine whether Bach1 is involved in the production of NO in macrophages, isolated macrophages were stimulated with or without LPS, and levels of NO were determined. The basal levels of NO production were comparable in control and *Bach1*$^{-/-}$ macrophages (Fig. 3). When stimulated with LPS, NO production was strongly induced in both macrophages, with no significant difference (Fig. 3). Since there is no report regarding HO-1 expression in *Bach1*-deficient macrophages, we examined LPS-induced HO-1 expression in peritoneal macrophages from *Bach1*$^{+/+}$ and control mice. Stimulation with LPS *ex vivo* increased HO-1 expression in *Bach1*$^{+/+}$ macrophages (Fig. 4). In contrast, HO-1 expression in macrophages from *Bach1*$^{-/-}$ mice was much higher than those from *Bach1*$^{+/+}$ mice even without LPS stimulation. Thus, it remains possible that overexpressed HO-1 modulates functions of *Bach1*-deficient macrophages other than the production of TNF-α and NO.

Effect of Bach1-deficiency on carrageenin - induced paw edema

As is the case of GalN/LPS-induced liver injury model,

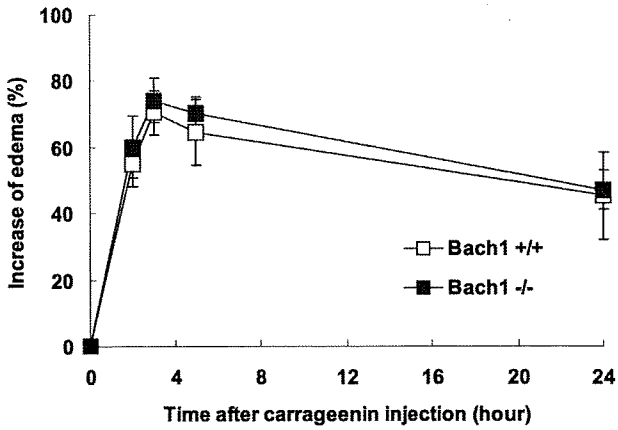

Fig. 5. Carrageenin-induced paw edema in control and *Bach1*$^{-/-}$ mice.
Paw volume was measured at 2, 3, 5 and 24 hours after carrageenin injection in control (open square) and *Bach1*$^{-/-}$ (closed square) mice. Data were calculated as percentage of increase of the paw volume by comparing pre- and post-carrageenin injection and shown as the mean ± SEM of five mice per group.

carrageenin-induced pleurisy is suppressed by induction of HO-1 (Willis et al. 1996). Thus, we next tested the effect of *Bach1*-deficiency in carrageenin-induced mouse paw edema as an inflammation model. However, there was no obvious difference in the progression of edematous injury between the two genotypes (Fig. 5). Thus, Bach1 may not be involved in the regulation of edematous response.

Discussion

Up-regulation of HO-1 by cobalt protoporphyrin is known to protect mice from apoptotic liver damage induced by GalN/LPS injection (Sass et al. 2003). In the present study, we examined effect of genetic ablation of Bach1 in this injury model system and found that Bach1 plays an inhibitory role in the protective response to this particular inflammatory stress *in vivo*. Specifically, induction of ALT and AST activities in blood was slightly suppressed in *Bach1*$^{+/-}$ mice, and more suppressed in *Bach1*$^{-/-}$ mice. Previously it was reported that LPS-induced liver injury is caused by hepatocyte apoptosis, mediated mainly by TNF-α (Morikawa et al. 1999). However, plasma TNF-α concentrations did not differ significantly between *Bach1*$^{+/+}$ and *Bach1*$^{-/-}$ mice. Furthermore, macrophages isolated from *Bach1*$^{-/-}$ mice produced similar levels of TNF-α compared to control macrophages when stimulated with LPS *in vitro*. Although we can not rule out the possibility that other changes in macrophages could potentially affect apoptosis of hepatic cells, Bach1-deficiency may affect hepatocyte function in a cell-autonomous manner as discussed below.

Because HO-1 is expressed at much higher levels in liver (Sun et al. 2002) and macrophages (this study) of *Bach1*-deficient mice, the observed cytoprotective effect of Bach1 ablation may involve HO-1 overexpression in these cells. The increased HO-1 expression caused by *Bach1*-deficiency is expected to lead to degradation of heme and generation of CO, ferrous iron, and biliverdin, which is rapidly reduced to bilirubin. CO is associated with inhibition of cell injury and vascular dilatation (Otterbein et al. 2003; Sass et al. 2003) and bilirubin exerts protection against oxidative cellular damage (Clark et al. 2000). While heme induces increased vascular permeability, adhesion molecule expression, and leukocyte recruitment, HO-1 antagonizes the heme-induced inflammation (Balla et al. 1991; Wagener et al. 2001). When taken together, it is conceivable that the protective effects caused by *Bach1*-deficiency in GalN/LPS-induced liver injury model reflect a composite mode of Bach1 action in hepatic cells and other cells including macrophages. It will be important to elucidate this complex network of cytoprotective responses at multiple levels.

Our previous (Omura et al. 2005; Yano et al. 2006) and current observations suggest that Bach1 inhibits cell and tissue survival in response to diverse stresses. Obvious enigma is whether Bach1 plays a role that allows natural selection inasmuch as natural selection usually favors a system for survival. Considering that heme is involved in a variety of biological events by modulating the function or the state of heme proteins (Furuyama et al. 2007), the primary function of Bach1 may reside in the regulation of heme homeostasis. Bach1 may also play beneficial roles as well in stress responses, which may have eluded our analysis thus far.

In contrast to the GalN/LPS-induced liver injury model, there was no protective effect of *Bach1*-deficiency in carrageenin-induced paw edema. Carrageenin, a water-extractable polysaccharide obtained from various seaweeds, induces macrophage accumulation in fluid exudates from subcutaneous chambers in dogs (Hou et al. 2004). Carrageenin activates kinin release and induces kinin B1 receptor (Campos et al. 1996; Decarie et al. 1996; Ni et al. 2003). Bradykinin, one of kinins, enhances vascular permeability and then causes inflammatory edema. It also activates phospholipase A2 (PLA2), enhancing PGE2 production which then enhances vascular permeability and vasodilation. Thrombin can act as an inflammatory mediator in this model (Cirino et al. 1996). Bach1 may not be related to these inflammatory mediators and to edematous response.

In conclusion, the results of this study suggest that Bach1 regulates the response of hepatic cells to inflammatory stresses. Taken together with its augmenting role in ischemic reperfusion injury of heart and atherosclerosis (Omura et al. 2005; Yano et al. 2006), inhibition of Bach1 may provide new therapeutic approaches toward various diseases.

Acknowledgements

We thank H. Suzuki, J. Sun, A. Muto and S. Omura for technical assistance. This work was supported in part by Grants-in-aid from the Ministry of Education, Science, Sport, and Culture of Japan.

References

Akagi, R., Takahashi, T. & Sassa, S. (2002) Fundamental role of heme oxygenase in the protection against ischemic acute renal failure. *Jpn. J. Pharmacol.*, **88**, 127-132.

Alam, J., Shibahara, S. & Smith, A. (1989) Transcriptional activation of the heme oxygenase gene by heme and cadmium in mouse hepatoma cells. *J. Biol. Chem.*, **264**, 6371-6375.

Amoutzias, GD., Veron, AS., Weiner, J., 3rd, Robinson-Rechavi, M., Bornberg-Bauer, E., Oliver, SG. & Robertson, DL. (2007) One billion years of bZIP transcription factor evolution: conservation and change in dimerization and DNA-binding site specificity. *Mol. Biol. Evol.*, **24**, 827-835.

Balla, G., Vercellotti, GM., Muller-Eberhard, U., Eaton, J. & Jacob, HS. (1991) Exposure of endothelial cells to free heme potentiates damage mediated by granulocytes and toxic oxygen species. *Lab, Inves.*, **64**, 648-655.

Baranano, D.E., Rao, M., Ferris, C.D. & Snyder, S.H. (2002) Biliverdin reductase: a major physiologic cytoprotectant. *Proc. Natl. Acad. Sci. USA*, **99**, 16093-16098.

Brouard, S., Otterbein, LE., Anrather, J., Tobiasch, E., Bach, FH., Choi, AM. & Soares, MP. (2000) Carbon monoxide generated by heme oxygenase 1 suppresses endothelial cell apoptosis. *J. Exp. Med.*, **192**, 1015-1026.

Campos, M.M., Souza, G.E. & Calixto, J.B. (1996) Upregulation of B1 receptor mediating des-Arg9-BK-induced rat paw oedema by systemic treatment with bacterial endotoxin. *Br. J. Pharmacol.*, **117**, 793-798.

Chen, K., Gunter, K. & Maines, M.D. (2000) Neurons overexpressing heme oxygenase-1 resist oxidative stress-mediated cell death. *J. Neurochem.*, **75**, 304-313.

Choi, A.M. & Alam, J. (1996) Heme oxygenase-1: function, regulation, and implication of a novel stress-inducible protein in oxidant-induced lung injury. *Am. J. Respir. Cell Mol. Biol.*, **15**, 9-19.

Cirino, G., Cicala, C., Bucci, M.R., Sorrentino, L., Maraganore, J.M. & Stone, S.R. (1996) Thrombin functions as an inflammatory mediator through activation of its receptor. *J. Exp. Med.*, **183**, 821-827.

Clark, J.E., Foresti, R., Sarathchandra, P., Kaur, H., Green, C.J. & Motterlini, R. (2000) Heme oxygenase-1-derived bilirubin ameliorates postischemic myocardial dysfunction. *Am. J. Physiol. Heart Circ. Physiol.*, **278**, H643-651.

Decarie, A., Adam, A. & Couture, R. (1996) Effects of captopril and Icatibant on bradykinin (BK) and des [Arg9] BK in carrageenan-induced edema. *Peptides*, **17**, 1009-1015.

Dorman, R.B., Bajt, M.L., Farhood, A., Mayes, J. & Jaeschke, H. (2004) Heme oxygenase-1 induction in hepatocytes and nonparenchymal cells protects against liver injury during endotoxemia. *Comp. Hepatol.*, **14 Suppl 1**, S42.

Furuyama, K., Kaneko, K. & Vargas, P.D. (2007) Heme as a magnificent molecule with multiple missions: heme determines its own fate and governs cellular homeostasis. *Tohoku J. Exp. Med.*, **213**, 1-16.

Hou, C., Kirchner, T., Singer, M., Matheis, M., Argentieri, D. & Cavender, D. (2004) In vivo activity of a phospholipase C inhibitor, 1-(6-((17beta-3-methoxyestra-1,3,5(10)-trien-17-yl)amino)hexyl)-1H-pyrrole-2,5-dione (U73122), in acute and chronic inflammatory reactions. *J. Pharmacol. Exp. Ther.*, **309**, 697-704.

Igarashi, K., Hoshino, H., Muto, A., Suwabe, N., Nishikawa, S., Nakauchi, H. & Yamamoto, M. (1998) Multivalent DNA binding complex generated by small Maf and Bach1 as a possible biochemical basis for beta-globin locus control region complex. *J. Biol. Chem.*, **273**, 11783-11790.

Igarashi, K. & Sun, J. (2006) The heme-Bach1 pathway in the regulation of oxidative stress response and erythroid differentiation. *Antioxid. Redox. Signal.*, **8**, 107-118.

Keyse, S.M. & Tyrrell, R.M. (1989) Heme oxygenase is the major 32-kDa stress protein induced in human skin fibroblasts by UVA radiation, hydrogen peroxide, and sodium arsenite. *Proc. Natl. Acad. Sci. USA*, **86**, 99-103.

Kyo, M., Yamamoto, T., Motohashi, H., Kamiya, T., Kuroita, T., Tanaka, T., Engel, J.D., Kawakami, B. & Yamamoto, M. (2004) Evaluation of MafG interaction with Maf recognition element arrays by surface plasmon resonance imaging technique. *Genes Cells.*, **9**, 153-164.

Lee, E.S., Ju, H.K., Moon, T.C., Lee, E., Jahng, Y., Lee, S.H., Son, J.K., Baek, S.H. & Chang, H.W. (2004) Inhibition of nitric oxide and tumor necrosis factor-alpha (TNF-alpha) production by propenone compound through blockade of nuclear factor (NF)-kappa B activation in cultured murine macrophages. *Biol. Pharm. Bull.*, **27**, 617-620.

Lehmann, V., Freudenberg, M.A. & Galanos, C. (1987) Lethal toxicity of lipopolysaccharide and tumor necrosis factor in normal and D-galactosamine-treated mice. *J. Exp. Med.*, **165**, 657-663.

Morikawa, A., Kato, Y., Sugiyama, T., Koide, N., Chakravortty, D., Yoshida, T. & Yokochi, T. (1999) Role of nitric oxide in lipopolysaccharide-induced hepatic injury in D-galactosamine-sensitized mice as an experimental endotoxic shock model. *Infect. Immun.*, **67**, 1018-1024.

Morikawa, A., Sugiyama, T., Kato, Y., Koide, N., Jiang, G.Z., Takahashi, K., Tamada, Y. & Yokochi, T. (1996) Apoptotic cell death in the response of D-galactosamine-sensitized mice to lipopolysaccharide as an experimental endotoxic shock model. *Infect. Immun.*, **64**, 734-738.

Motohashi, H., O'Connor, T., Katsuoka, F., Engel, J.D. & Yamamoto, M. (2002) Integration and diversity of the regulatory network composed of Maf and CNC families of transcription factors. *Gene*, **294**, 1-12.

Nakahira, K., Takahashi, T., Shimizu, H., Maeshima, K., Uehara, K., Fujii, H., Nakatsuka, H., Yokoyama, M., Akagi, R. & Morita, K. (2003) Protective role of heme oxygenase-1 induction in carbon tetrachloride-induced hepatotoxicity. *Biochem. Pharmacol.*, **66**, 1091-1105.

Ni, A., Yin, H., Agata, J., Yang, Z., Chao, L. & Chao, J. (2003) Overexpression of kinin B1 receptors induces hypertensive response to des-Arg9-bradykinin and susceptibility to inflammation. *J. Biol. Chem.*, **278**, 219-225.

Ogawa, K., Sun, J., Taketani, S., Nakajima, O., Nishitani, C., Sassa, S., Hayashi, N., Yamamoto, M., Shibahara, S., Fujita, H. & Igarashi, K. (2001) Heme mediates derepression of Maf recognition element through direct binding to transcription repressor Bach1. *EMBO J.*, **20**, 2835-2843.

Omura, S., Suzuki, H., Toyofuku, M., Ozono, R., Kohno, N. & Igarashi, K. (2005) Effects of genetic ablation of bach1 upon smooth muscle cell proliferation and atherosclerosis after cuff injury. *Genes Cells.*, **10**, 277-285.

Otterbein, L.E., Zuckerbraun, B.S., Haga, M., Liu, F., Song, R., Usheva, A., Stachulak, C., Bodyak, N., Smith, R.N., Csizmadia, E., Tyagi, S., Akamatsu, Y., Flavell, R.J., Billiar, T.R., Tzeng, E., Bach, F.H., Choi, A.M. & Soares, M.P. (2003) Carbon monoxide suppresses arteriosclerotic lesions associated with chronic graft rejection and with balloon injury. *Nat. Med.*, **9**, 183-190.

Oyake, T., Itoh, K., Motohashi, H., Hayashi, N., Hoshino, H., Nishizawa, M., Yamamoto, M. & Igarashi, K. (1996) Bach proteins belong to a novel family of BTB-basic leucine zipper transcription factors that interact with MafK and regulate transcription through the NF-E2 site. *Mol. Cell. Biol.*, **16**, 6083-6095.

Petrache, I., Otterbein, L.E., Alam, J., Wiegand, G.W. & Choi, A.M. (2000) Heme oxygenase-1 inhibits TNF-alpha-induced apoptosis in cultured fibroblasts. *Am. J. Physiol. Lung Cell Mol. Physiol.*, **278**, L312-319.

Poss, K.D. & Tonegawa, S. (1997a) Heme oxygenase 1 is required for mammalian iron reutilization. *Proc. Natl. Acad. Sci. USA.*,

94, 10919-10924.

Poss, K.D. & Tonegawa, S. (1997b) Reduced stress defense in heme oxygenase 1-deficient cells. *Proc. Natl. Acad. Sci. USA.*, **94**, 10925-10930.

Sass, G., Soares, MC., Yamashita, K., Seyfried, S., Zimmermann, W.H., Eschenhagen, T., Kaczmarek, E., Ritter, T., Volk, H.D. & Tiegs, G. (2003) Heme oxygenase-1 and its reaction product, carbon monoxide, prevent inflammation-related apoptotic liver damage in mice. *Hepatology*, **38**, 909-918.

Shibahara, S., Muller, R., Taguchi, H. & Yoshida, T. (1985) Cloning and expression of cDNA for rat heme oxygenase. *Proc. Natl. Acad. Sci. USA*, **82**, 7865-7869.

Shibahara, S., Muller, R.M. & Taguchi, H. (1987) Transcriptional control of rat heme oxygenase by heat shock. *J. Biol. Chem.*, **262**, 12889-12892.

Shimizu, H., Takahashi, T., Suzuki, T., Yamasaki, A., Fujiwara, T., Odaka, Y., Hirakawa, M., Fujita, H. & Akagi, R. (2000) Protective effect of heme oxygenase induction in ischemic acute renal failure. *Crit. Care Med.*, **28**, 809-817.

Sun, J., Hoshino, H., Takaku, K., Nakajima, O., Muto, A., Suzuki, H., Tashiro, S., Takahashi, S., Shibahara, S., Alam, J., Taketo, MM., Yamamoto, M. & Igarashi, K. (2002) Hemoprotein Bach1 regulates enhancer availability of heme oxygenase-1 gene. *EMBO J.*, **21**, 5216-5224.

Sun, J., Brand, M., Zenke, Y., Tashiro, S., Groudine, M. & Igarashi, K. (2004) Heme regulates the dynamic exchange of Bach1 and NF-E2-related factors in the Maf transcription factor network. *Proc. Natl. Acad. Sci. USA.*, **101**, 1461-1466.

Suzuki, H., Tashiro, S., Hira, S., Sun, J., Yamazaki, C., Zenke, Y., Ikeda-Saito, M., Yoshida, M. & Igarashi, K. (2004) Heme regulates gene expression by triggering Crm1-dependent nuclear export of Bach1. *EMBO J.*, **23**, 2544-2553.

Taketani, S., Kohno, H., Yoshinaga, T. & Tokunaga, R. (1989) The human 32-kDa stress protein induced by exposure to arsenite and cadmium ions is heme oxygenase. *FEBS Lett.*, **245**, 173-176.

Tiegs, G., Wolter, M. & Wendel, A. (1989) Tumor necrosis factor is a terminal mediator in galactosamine/endotoxin-induced hepatitis in mice. *Biochem. Pharmacol.*, **38**, 627-631.

Wagener, FA., Eggert, A., Boerman, OC., Oyen, WJ., Verhofstad, A., Abraham, NG., Adema, G., van Kooyk, Y., de Witte, T. & Figdor, CG. (2001) Heme is a potent inducer of inflammation in mice and is counteracted by heme oxygenase. *Blood*, **98**, 1802-1811.

Wang, M.H., Cox, G.W., Yoshimura, T., Sheffler, L.A., Skeel, A. & Leonard, E.J. (1994) Macrophage-stimulating protein inhibits induction of nitric oxide production by endotoxin- or cytokine-stimulated mouse macrophages. *J. Biol. Chem.*, **269**, 14027-14031.

Willis, D., Moore, A.R., Frederick, R. & Willoughby, D.A. (1996) Heme oxygenase: a novel target for the modulation of the inflammatory response. *Nat. Med.*, **2**, 87-90.

Wolf, A.M., Wolf, D., Rumpold, H., Ludwiczek, S., Enrich, B., Gastl, G., Weiss, G. & Tilg, H. (2005) The kinase inhibitor imatinib mesylate inhibits TNF-{alpha} production in vitro and prevents TNF-dependent acute hepatic inflammation. *Proc. Natl. Acad. Sci. USA.*, **102**, 13622-13627.

Yachie, A., Niida, Y., Wada, T., Igarashi, N., Kaneda, H., Toma, T., Ohta, K., Kasahara, Y. & Koizumi, S. (1999) Oxidative stress causes enhanced endothelial cell injury in human heme oxygenase-1 deficiency. *J. Clin. Invest.*, **103**, 129-135.

Yang, L., Quan, S. & Abraham, N.G. (1999) Retrovirus-mediated HO gene transfer into endothelial cells protects against oxidant-induced injury. *Am. J. Physiol.*, **277**, L127-133.

Yano, Y., Ozono, R., Oishi, Y., Kambe, M., Yoshizumi, M., Ishida, T., Omura, S., Oshima, T. & Igarashi, K. (2006) Genetic ablation of the transcription repressor Bach1 leads to myocardial protection against ischemia/reperfusion in mice. *Genes Cells*, **11**, 791-803.

Zenke-Kawasaki, Y., Dohi, Y., Katoh, Y., Ikura, T., Ikura, M., Asahara, T., Tokunaga, F., Iwai, K. & Igarashi, K. (2007) Heme induces ubiquitination and degradation of the transcription factor Bach1. *Mol. Cell. Biol.*, **27**, 6962-6971.

Hepatocyte growth factor in transient myeloproliferative disorder of Down syndrome

Keiichi Hirono,[1] Masayoshi Miura,[2] Hirokazu Kanegane,[1] Masatoshi Miyamoto,[3] Naoki Yoshimura,[4] Fukiko Ichida,[1] Etsuro Ito[5] and Toshio Miyawaki[1]

[1]*Department of Pediatrics and* [4]*First Department of Surgery, Graduate School of Medicine, University of Toyama, Departments of* [2]*Pediatrics and* [3]*Pediatric Surgery, Toyama City Hospital, Toyama and* [5]*Department of Pediatrics, Hirosaki University School of Medicine, Hirosaki, Japan*

Key words Down syndrome, hepatocyte growth factor, transient myeloproriferative disorder.

Transient myeloproliferative disorder (TMD), also known as transient abnormal myelopoiesis, occurs in approximately 10% of neonates with Down syndrome (DS).[1,2] Although most patients with TMD spontaneously undergo remission, the disease sometimes results in severe or lethal hydrops fetalis, multiple effusions, and liver or multi-organ failure. Pericardial, ascetic, or pleural effusions are commonly found in DS-TMD.[3] The causative mechanism of pericardial effusions in DS-TMD, however, remains unclear. Hepatocyte growth factor (HGF) is a mesenchyme-derived pleiotropic factor that controls the proliferation of endothelial cells, and also acts as a multifunctional cytokine, explaining its function in organogenesis and tissue regeneration.[4,5] We show that HGF levels are elevated in serum and pericardial fluid during TMD, especially in pericardial fluid, and are decreased with the disease's regression following steroid therapy. HGF may play some role in the pathogenesis of DS-TMD.

Case report

A 1-day-old male infant was admitted to hospital because of vomiting and hyperleukocytosis. His mother, who was 30 years old, had an uneventful pregnancy and delivery. His birthweight was 2610 g. Physical examination showed characteristic signs of DS, later confirmed on chromosomal analysis. The liver and spleen were palpable 5 cm below the costal margins. Lymph node swelling, and bruising or petechiae were not detected. A radiogram and an echocardiogram disclosed congenital duodenal obstruction and an atrial septal defect. Pericardial effusion was not observed on echography on admission. On complete blood cell count hemoglobin level was 14.5 g/dL, platelet count was $94.0 \times 10^3/\mu L$ and leukocyte count was $363.2 \times 10^3/\mu L$, with 49.5% blasts. The blast cells had a high nucleus to cytoplasmic ratio, round nuclei with indistinct nucleoli, and a basophilic cytoplasm without azurophilic granules. Some of them had cytoplasmic budding. The blasts were negative for myeloperoxidase and positive for CD7, CD34, CD38, CD41a, and CD61, indicating that they seemed to be megakaryocytic in nature. Bone marrow aspiration indicated hypocellular marrow with an excess of blasts. A chromosomal study of the blasts showed trisomy 21 without other clonal chromosomes. The patient was diagnosed as having TMD.

Direct sequencing indicated a 129-nucleotide deletion (342–470). This mutation led to an internal deletion of 43 amino acids (codons 77–119) in the *N*-terminal activation domain. In most cases of TMD the mutation in the *GATA1* gene leads to expression of GATA1 lacking the *N*-terminal activation domain (codons 1–83). This patient was the second TMD patient with identical internal deletion.[6]

The side-to-side duodenostomy was performed at 2 days of age, and showed a classic annular pancreas with an underlying duodenal stenosis. At 6 days of age cardiomegaly with pericardial effusion was detected on echocardiography. Pericardiocentesis was performed, and 5 mL of pericardial fluid was drained. The pericardial fluid was clear, yellowish, and exudative, but no mesothelial cells, macrophages, or inflammatory cells were detected. At 9 days of age dexamethazone (0.5 mg/kg) was administered for 3 days, and the pericardial effusion diminished in 1 month (Fig. 1). Although the blast cell count gradually decreased after steroid treatment, it subsequently increased (Fig. 1). This was accompanied by elevated levels of serum liver enzymes, collagen IV, and hyaluronic acid, with jaundice, suggesting progressive hepatic fibrosis. Low doses of cytosine arabinoside (Ara-C; 10 mg/m^2, once a day) were administered for 7 days, which resulted in remission (Fig. 1). This was accompanied by recovery of cardiac function. Peripheral blasts had completely disappeared by 55 days of age, which was accompanied by a recovery of hematopoiesis. An operation for the cardiac defect is contemplated, and cardiac function has returned to normal.

Concentration levels of HGF in pericardial fluid and serum

Samples of pericardial fluid were obtained immediately after incision of pericardium. Peripheral blood samples were taken from the patient at the same time. The samples were collected in tubes, centrifuged at 3000 *g* for 10 min at 4°C, and frozen at −80°C until measurement. HGF concentrations were measured using an ELISA kit (R&D Systems, Minneapolis, MN, USA).

The HGF levels in serum and pericardial fluid were significantly elevated before steroid treatment, and decreased after the

Correspondence: Keiichi Hirono, MD, Department of Pediatrics, Graduate School of Medicine, University of Toyama, 2630 Sugitani, Toyama 930-0194, Japan. Email: khirono-circ@umin.ac.jp

Received 3 May 2007; revised 9 October 2007; accept 21 January 2008.
doi: 10.1111/j.1442-200X.2009.02897.x

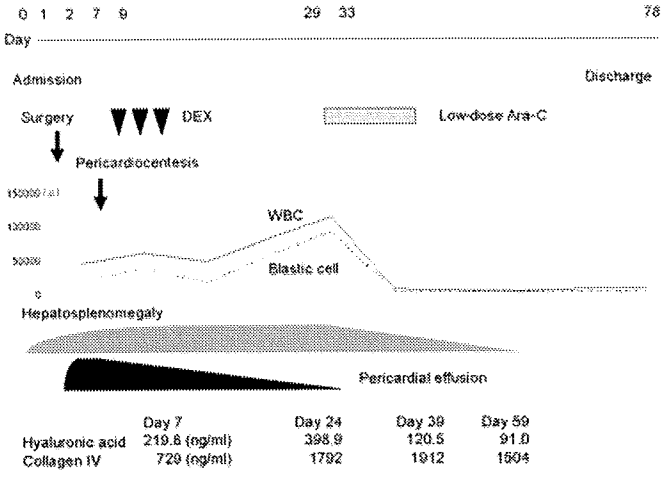

Fig. 1 Clinical course. Ara-C, cytosine arabinoside; DEX, dexamethasone; WBC, white blood cell.

treatment: the concentration of HGF was increased more in pericardial fluid than in serum (Table 1).[7,8]

Discussion

Transient myeloproliferative disorder, also known as transient abnormal myelopoiesis or transient leukemia, occurs in approximately 10% of neonates with DS.[1,2] Many infants with TMD are clinically well with an incidental finding of circulating blasts, and usually undergo spontaneous remission. In some cases, however, the disease is severe and potentially lethal, presenting with hydrops fetalis, multiple effusions, and liver or multi-organ system failure.[9–11] Pericardial, ascetic, or pleural effusion has been found in 10 of 48 cases (21%) of DS-TMD.[2] The causative mechanism, however, has not been fully studied and little is known of the real incidence of pericardial effusion in DS. In the present case pericardial effusion was not observed at birth, but became evident as the blastic cells proliferated (Fig. 1). The pericardial effusion decreased after steroid treatment, and had disappeared in approximately 1 month, when low-dose Ara-C was given. The patient had moderate left-to-right shunt of atrial septal defect but his cardiac function remained normal. Thus, his fluid administration volume was approximately 80% lower than for a normal baby, even when he was treated with Ara-C. The pericardial fluid was exudative but had no cells. These findings suggested that the occurrence of pericardial effusion was correlated with the progression of TMD without the pericardium's invasion by blast cells.

Table 1 Concentration of HGF (pg/mL)

	Steroid treatment (dexamethazone (0.5 mg/kg) for 3 days)	
	Before treatment (Day 7)	After treatment (Day 170)
Pericardial fluid	7534	51
Serum	4765	3227

Serum HGF levels of control: 1283 – 1000 pg/mL.

Down syndrome–TMD has been reported to be associated with abnormal inflammatory cytokinemia such as tumor necrosis factor-α, interleukin-1β and interferon-γ.[12] In contrast, HGF is a pleiotropic factor derived from mesenchymal tissue, and it controls endothelial cell proliferation.[3] HGF is also a multifunctional cytokine, which explains its function in organogenesis and tissue regeneration. It was considered that the sustained pro-inflammatory cytokinemia and imperfect remodeling might induce liver fibrosis in fatal TMD. We found that concentrations of HGF are elevated in serum and pericardial fluid during the TMD phase, especially in pericardial fluid, and decreased following steroid therapy. An elevated level of HGF in the serum might reflect the occurrence of cholestasis and hepatic fibrosis with TMD.[4] It is proposed that HGF plays an important role in the excess production of pericardial fluid and focal angiogenesis in the pericardium because HGF could stimulate blood vessel formation, cell proliferation, invasion, and motility.

In conclusion, we showed that HGF levels are elevated in serum and pericardial fluid in cases of DS-TMD. HGF may play a role in the pathogenesis of DS-TMD. Further investigation is required to clarify the role of HGF in pericardial fluid and serum during TMD.

References

1 Zipursky A. The treatment of children with acute megakaryoblastic leukemia who have Down syndrome. *Pediatr. Hematol. Oncol.* 1996; **18**: 10–12.
2 Zipursky A, Brown EJ, Christensen H, Doyle J. Transient myeloproliferative disorder (transient leukemia) and the hematologic manifestations of Down syndrome. *Clin. Lab. Med.* 1999; **19**: 157–67.
3 Massey GV, Zipursky A, Chang MN *et al.* A prospective study of the natural history of transient leukemia (TL) in neonates with Down syndrome (DS): Children's Oncology Group (COG) study POG-9481. *Blood* 2006; **107**: 4606–13.
4 Matsumoto K, Nakamura T. Emerging multipotent aspects of hepatocyte growth factor. *J. Biochem.* 1996; **111**: 591–600.
5 Gohda E, Nakamura S, Yamamoto I, Minowada J. Hepatocyte growth factor: Pleiotropic cytokine produced by human leukemia cells. *Leuk. Lymphoma* 1995; **19**: 197–205.
6 Xu G, Nagano M, Kanezaki R *et al.* Frequent mutations in the GATA-1 gene in the transient myeloproliferative disorder of Down syndrome. *Blood* 2003; **102**: 2960–68.
7 Shiota G, Okano J, Kawasaki H *et al.* Serum hepatocyte growth factor levels in liver diseases: Clinical implications. *Hepatology* 1995; **21**: 106–12.
8 Nakamura S, Gohda E, Matsuo Y *et al.* Significant amount of hepatocyte growth factor detected in blood and bone marrow plasma of leukaemia patients. *Br. J. Haematol.* 1994; **87**: 640–42.
9 Weinstein HJ. Congenital leukemia and the neonatal myeloproliferative disorders associated with Down syndrome: A report. *Clin. Haematol.* 1978; **7**: 147–54.
10 Al-Kasim F, Doyle JJ, Massey GV, Weinstein HJ, Zipursky A; Pediatric Oncology Group. Incidence and treatment of potentially lethal diseases in transient leukemia of Down syndrome: Pediatric Oncology Group study. *J. Pediatr. Hematol. Oncol.* 2002; **25**: 9–13.
11 Issacs H. Fetal and neonatal leukemia. *J. Pediatr. Hematol. Oncol.* 2003; **25**: 348–61.
12 Shimada A, Hayashi Y, Ogasawara M *et al.* Pro-inflammatory cytokinemia is frequently found in Down syndrome patients with hematological disorders. *Leuk. Res.* 2007; **31**: 1199–203.

Clin Exp Nephrol (2009) 13:508–511
DOI 10.1007/s10157-009-0178-2

CASE REPORT

A boy with membranous nephropathy after allogeneic bone marrow transplantation

Osamu Motoyama · Yumiko Uchino · Mika Tokuyama · Kikuo Iitaka · Akira Ohara

Received: 12 November 2008 / Accepted: 11 March 2009 / Published online: 9 May 2009

Abstract A 6-year-old boy developed bronchiolitis obliterans organizing pneumonia and nephrotic syndrome 5 months after allogeneic bone marrow transplantation from an unrelated donor for acute lymphoblastic leukemia. His renal biopsy showed membranous nephropathy. He was treated with prednisolone and cyclosporine A. Proteinuria disappeared 3 months after the onset of nephrotic syndrome. To our knowledge, this patient is the youngest case with nephrotic syndrome due to membranous nephropathy after hematopoietic stem cell transplantation.

Keywords Bone marrow transplantation · Graft-versus-host disease · Hematopoietic stem cell transplantation · Membranous nephropathy · Nephrotic syndrome

Introduction

Nephrotic syndrome (NS) associated with chronic graft-versus-host disease (GVHD) after hematopoietic stem cell transplantation (HSCT) has been reported [1–23]. Membranous nephropathy (MN) after HSCT occurred mainly in adults and minimal change nephrotic syndrome (MCNS) in children [10]. To our knowledge, only one child under 15 years of age with NS due to MN after HSCT has been reported previously [3].

O. Motoyama (✉) · M. Tokuyama
Department of Pediatrics, Toho University Medical Center, Sakura Hospital, 564-1 Shimoshizu, Sakura Chiba 285-8741, Japan
e-mail: motoyan@basil.ocn.ne.jp

Y. Uchino · A. Ohara
Department of Pediatrics, Toho University Medical Center, Omori Hospital, Tokyo, Japan

K. Iitaka
Department of Pediatrics, Social Insurance Sagamino Hospital, Kanagawa, Japan

Case report

A 5-year-old boy was noted to have peripheral blood white cell count of 62,900/μl, containing 70% of blast cells, when he visited a clinic for a bruise on his face. Nuclear cells of bone marrow were 860,000/μl, and 94% were blast cells. In February 2002, he was diagnosed as having acute Philadelphia positive B cell lymphoblastic leukemia. He was treated with prednisolone (PSL), vincristine, cyclophosphamide, etc., and went into complete remission. Seven months after the onset of leukemia, allogeneic bone marrow transplantation (BMT) from an HLA-matched unrelated donor was successfully performed. His HLA was A2, A26, B46, B61, C1 and C9. Pre-transplant treatment included etoposide, cyclophosphamide and total body irradiation. For prophylaxis of acute GVHD, methotrexate was administered four times for 12 days, and a trough level of tacrolimus was maintained between 6 and 12 ng/ml after BMT. Ten days later, fever and generalized erythema occurred, and grade II acute GVHD was diagnosed [24]. He was treated with a single dose of high-dose methylprednisolone (25 mg/kg). Granulocytes were over 500/μl at 20 days and thrombocytes over 50,000/μl at 36 days after BMT. Tacrolimus was withdrawn 3 months after BMT. Four months after BMT, a skin eruption and elevated serum aspartate aminotransferase (114 IU/l: normal 12–35 IU/l) were noted, and chronic GVHD of the skin and liver was diagnosed. He developed tachypnea with hypoxemia. Chest X-ray film showed diffuse nodular lesions. Pulmonary

function test revealed obstructive and constrictive respiratory dysfunction. He was diagnosed as having bronchiolitis obliterans organizing pneumonia related to chronic GVHD. He was treated with high-dose methylprednisolone (18 mg/kg per day for 3 days), followed by PSL (0.5 mg/kg per day). Dyspnea improved 3 days after treatment. The skin eruption and hepatic dysfunction also improved gradually. In February 2003, 5 months after BMT when he was 6 years old, he developed microscopic hematuria (16–20 red blood cells/high-power field) and proteinuria. He became nephrotic, with total protein 5.1 g/dl, albumin 1.9 g/dl, total cholesterol 554 mg/dl and proteinuria 4.7 g/day. Blood pressure and renal function were normal with serum creatinine of 0.2 mg/dl. Serum levels of CH50, C3, C4 and IgE were normal. Surface antigen of hepatitis B virus, antibody against hepatitis C virus, anti-nuclear antibody and anti-DNA antibody were negative. Renal biopsy was performed. Thirty-six glomeruli were obtained and showed only mild capillary wall thickness. Spike formation was not observed on periodic acid-methenamine staining (Fig. 1a). There were no tubulo-interstitial or vascular changes. Deposits of IgG, C3, C4 and C1q along the capillary walls were observed on immunofluorescent microscopy (Fig. 1b). Numerous subepithelial electron-dense deposits were noted on electron microscopy (Fig. 1c). MN stage 2 was diagnosed [25]. He was treated with PSL (1 mg/kg per day) and cyclosporine A (CyA) to keep a whole blood trough level of 100–150 ng/ml. PSL was reduced gradually for 5 months and was then withdrawn. CyA was maintained for 10 months. Proteinuria disappeared 3 months after the start of treatment for NS, but microscopic hematuria continued for 5 years after the onset of NS, when he was 12 years old. A CD4/CD8 ratio of T-cells was 0.7–0.8 during NS, and this was within the normal range of 0.6–2.9.

Discussion

Renal involvement after HSCT is known as HSCT-related nephropathy. The conditioning regimen for HSCT consists of high-dose cytotoxic chemotherapy and total body irradiation, which can cause acute and chronic renal failure due to thrombotic microangiopathy, tubulointerstitial damage and radiation nephropathy. NS usually occurs at the late phase in 0.5–1.8% of patients receiving HSCT [6, 13, 14] and is thought to be GVHD-related nephropathy. Chronic GVHD is a multi-organ disease that occurs after about 100 days following HSCT, mainly affecting the skin, liver, eyes, mouth, upper respiratory tract and esophagus. It is thought to be associated with activation of the immune system, and clinical manifestations resemble the changes of autoimmune diseases.

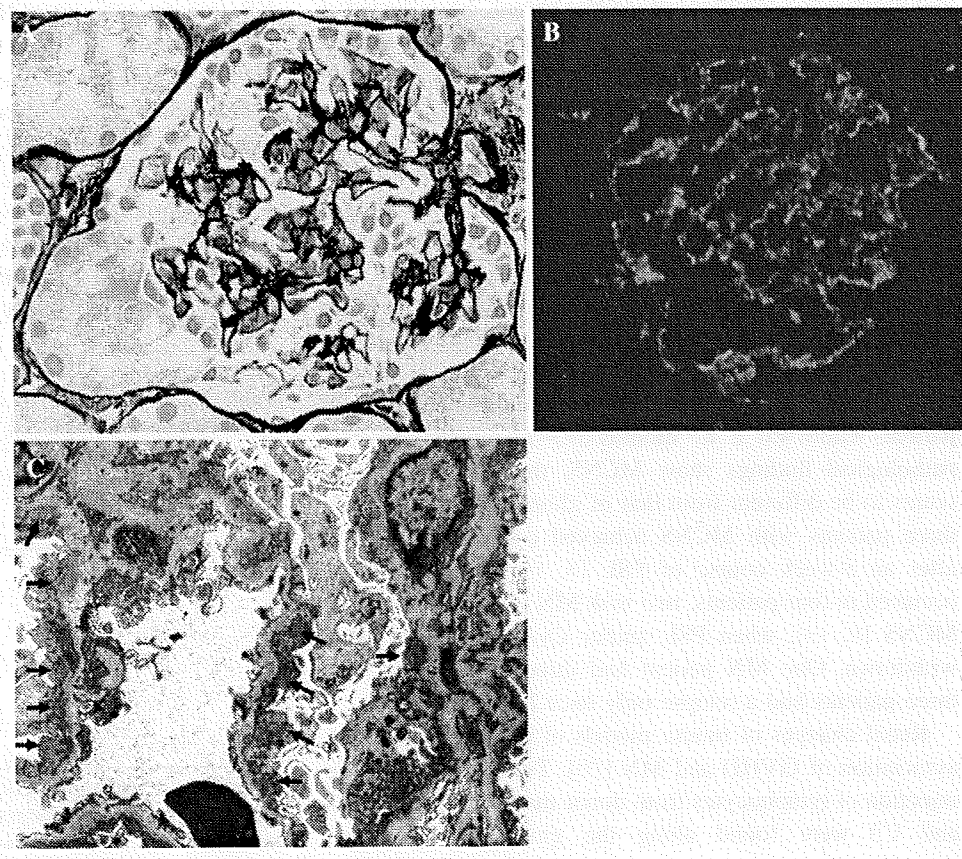

Fig. 1 **a** Light micrograph showing mild thickening of glomerular capillary walls without spike formation. Periodic acid-silver methenamine stain, ×200. **b** Immunofluorescent micrograph showing deposition of IgG along glomerular capillaries. **c** Electron micrograph showing numerous electron-dense deposits (*arrows*) in the subepithelial region and slightly irregular basement membrane with small spikes over the entire circumference of the capillaries, ×2,000